Check for updates

Hydrological Processes

WILEY

RESEARCH ARTICLE OPEN ACCESS

Tracing Seasonal Ground Thaw with Stream Chemistry in Alaskan Arctic Permafrost Catchments

Amelia L. Grose[1] | Jay P. Zarnetske[1] | Arsh Grewal[2] | Arial J. Shogren[3] | Abigail F. Rec[4] | Jonathan A. O'Donnell[5] | Benjamin W. Abbott[6] | William B. Bowden[4]

[1]Department of Earth and Environmental Sciences, Michigan State University, East Lansing, Michigan, USA | [2]Department of Geography and Planning, University of Saskatchewan, Saskatoon, Saskatchewan, Canada | [3]Department of Biological Sciences, The University of Alabama, Tuscaloosa, Alabama, USA | [4]Rubenstein School of Environment and Natural Resources, University of Vermont, Burlington, Vermont, USA | [5]National Park Service, Arctic Network, Anchorage, Alaska, USA | [6]Department of Plant and Wildlife Sciences, Brigham Young University, Provo, Utah, USA

Correspondence: Amelia L. Grose (groseame@msu.edu)

Received: 26 September 2025 | **Revised:** 23 March 2026 | **Accepted:** 26 March 2026

Keywords: active layer | Arctic | concentration–discharge | ground thaw | permafrost | tracers

ABSTRACT

In permafrost regions, hydrological and biogeochemical processes are substantially influenced by ground thaw dynamics. However, seasonal and interannual changes in ground thaw are difficult to measure at catchment and regional scales. Prior studies have used stream chemistry to indicate water flowpaths at catchment scales by taking advantage of vertical differences in solute sources, but the consistency of these chemical tracers across varying Arctic landscapes is poorly understood. In this study, we analysed nine potential thaw depth tracers (Ba, Ca, Fe, K, Mg, Na, S, Si and Sr) for three consecutive thaw seasons (June through early September, 2021–2023) across three catchments with different landscape characteristics in the continuous permafrost region of northern Alaska, United States. We used generalised additive models to test which solutes made effective tracers of thaw depth across catchments, based on significant concentration–discharge relationships and seasonality. Five solutes met the criteria for an effective thaw tracer in at least one catchment, but there was no single tracer that worked across all three catchments, with the differences likely due to variation in catchment characteristics (e.g., geology, soils, lake coverage). Tracking ground thaw dynamics via stream chemistry is a promising approach that complements modelling and point measurements of thaw by filling gaps in spatial and temporal scales. Overcoming the current limitations of observing ground thaw across spatial scales, seasons and years is needed as thaw dynamics will become increasingly important in Arctic systems experiencing both warming and hydrologic intensification.

1 | Introduction

Permafrost, which is ground that has been frozen for at least two consecutive years, underlies 15% of the exposed land surface in the northern hemisphere (Obu 2021) and stores around 1500 Pg of organic carbon (Schuur et al. 2022) as well as other nutrients, ions and metals (Colombo et al. 2018; Reyes and Lougheed 2015; Skierszkan, Dockrey, and Lindsay 2024). Permafrost acts as a practically impermeable barrier across most of the Arctic, restricting water flowpaths to the near-surface (Dingman 1973; Lafrenière and Lamoureux 2019; Quinton and Marsh 1999; Woo 1983).

The Arctic is warming four times faster than the global average (Rantanen et al. 2022), leading to distinct changes in hydrological and biogeochemical cycles in the region. Warming temperatures are resulting in increased overall precipitation, with a smaller proportion falling as snow (Bintanja and Andry 2017). Additionally, permafrost thaw is leading to dampened runoff response and weaker freshet, largely due to increases in water

This is an open access article under the terms of the Creative Commons Attribution License, which permits use, distribution and reproduction in any medium, provided the original work is properly cited.

© 2026 The Author(s). *Hydrological Processes* published by John Wiley & Sons Ltd.

storage capacity (Bring et al. 2016; Koch et al. 2022). Shifting precipitation regimes and permafrost thaw are resulting in increased subsurface flow, baseflow and annual streamflow (Arp et al. 2020; Michalek et al. 2025; Rawlins and Karmalkar 2024). It is widely expected that increasing permafrost thaw will allow deeper flowpaths to access previously frozen soil, transporting formerly trapped carbon, nutrients, ions and metals to nearby streams (Frey and McClelland 2009; Frey et al. 2007; O'Donnell et al. 2024; Tank et al. 2023; Toohey et al. 2016).

Seasonal conditions, including catchment wetness and thermal status of the soil layer above the permafrost table (known as the 'active layer'), also control dominant flowpaths (Chiasson-Poirier et al. 2020; O'Connor et al. 2019; Woo 1983; Woo et al. 1981; Woo and Steer 1983). During high flows and frozen ground conditions, shallow flowpaths dominate, while deeper flowpaths near the permafrost table are more active during low flows and late in the thaw season (Hinzman et al. 1991; King et al. 2020; Woo 1983; Woo and Steer 1982; Woo and Steer 1986). Strong seasonality in ground thaw and the phase and magnitude of precipitation lead to strong seasonality in dominant flowpaths. In the spring, infiltration of a large volume of snowmelt is restricted by the frozen active layer, leading to rapid transmission of water as overland flow and very shallow subsurface flow (Hinzman et al. 1991; Lewkowicz and French 1982; McNamara et al. 1997; Woo 1983, 1986; Woo and Steer 1982). As snowmelt ceases and the thaw front descends, storage capacity increases and deeper flowpaths are activated (Carey and Woo 1999; Chiasson-Poirier et al. 2020; McNamara et al. 1997; Woo 1983). The ground continues to thaw down to the top of the permafrost table, which is effectively the 'bottom' of the catchment (Condon et al. 2020) as the water stored within and below permafrost is largely disconnected from mobile storage, except in cases where springs from deep regional aquifers enter river valleys (Kane et al. 2013; Koch et al. 2024).

Active layer thickness, or maximum annual thaw depth, is increasing or predicted to increase in much of the Arctic in response to climate warming, shifting precipitation regimes and changing soil thermal properties which are impacted by depth of the organic horizon and moisture (Anisimov et al. 1997; Clayton et al. 2021; Kane et al. 1991; Luo et al. 2016; Walvoord and Kurylyk 2016). It is necessary to understand not only the maximum depth of thaw in the thaw season, but also the timing of seasonal ground thaw, as flowpath depth impacts the amount and form of nutrients and other solutes transported to aquatic ecosystems (Frey and McClelland 2009; Harms and Jones Jr. 2012; Striegl et al. 2005; Vonk et al. 2015). For example, thaw depth may impact nitrogen dynamics in soils and streams, as deeper flowpaths through inorganic soil horizons can promote nitrogen mineralisation and export in its inorganic form (Harms and Jones Jr. 2012; Khosh et al. 2017). As inorganic nitrogen is one of the limiting nutrients in Arctic ecosystems, changes in thaw depth can have ecosystem-level impacts (Myrstener et al. 2018; Shaver and Chapin 1980; Shaver et al. 1986). Therefore, active layer dynamics are a key control on hydrologic and ecosystem conditions in permafrost regions.

Measuring active layer dynamics and permafrost table depth across space and time remains logistically challenging. Current methods include thaw depth surveys via direct depth-to-resistance probing, which are time-consuming, better suited for small scales ($<1\,km^2$) and lack accuracy in rocky terrain (Boike et al. 2022). Advances have been made in remote sensing and modelling that allow for detection of general thaw depth in a region; however, these face difficulties in capturing spatial variability and precision (Chen et al. 2020; Westermann et al. 2015). Studies have also used streamflow recession to understand changes in thaw depth, but this approach relies on the occurrence of distinct event runoff responses throughout the ice-free season, resulting in missing information in years when these distinct events do not occur (Cooper et al. 2023; Hinzman et al. 2020; McNamara et al. 1998).

Stream networks may be used as sensors of landscape processes, as they integrate chemical signals vertically and laterally throughout catchments (Johnson et al. 1997; Shogren et al. 2019; Stewart et al. 2022). This integration is mediated by hydrologic connectivity, as contributing areas to streams are often constrained to near-stream zones that can differ in solute concentrations from upslope soils (Blackburn et al. 2017; Knapp et al. 2022; Ledesma et al. 2018). Stream chemistry reflects water sources and flowpaths, with variation in solutes delivered to the stream according to the contributing areas as well as the depth of the flowpaths through the hillslope (Stewart et al. 2022). The 'shallow and deep hypothesis' describes the concept that stream chemistry is determined by water flowpaths, which are dependent on discharge (Stewart et al. 2022; Zhi et al. 2019; Zhi and Li 2020). The hypothesis focuses on vertical heterogeneity in solutes and flowpaths, indicating that deeper subsurface chemistry is reflected in the stream during baseflows, whereas shallower subsurface chemistry is reflected during high flows. Therefore, solutes that increase in concentration with depth in the soil profile are diluted in the stream at high flows, while those that are abundant near the surface show opposite, flushing patterns (Stewart et al. 2022; Zhi and Li 2020; Zhi et al. 2019). Horizontal heterogeneity in the landscape can also impact solute concentrations, especially during storms when the contributing area to the stream extends from the nearby riparian areas (Dunne and Black 1970; Spence et al. 2010). In the Arctic, changes in flowpaths are not only impacted by variations in discharge, but also changes in subsurface storage as the active layer thaws throughout the summer. Although developed in temperate catchments, the 'shallow and deep hypothesis' may be useful for documenting shifting flowpath depths in permafrost catchments (e.g., Carey et al. 2013). Whil seasonality in evapotranspiration (ET) can also influence discharge and dominant flowpaths, it is unlikely to directly influence dominant flowpaths in tundra environments over the short term. Recent work in similar tundra environments has shown that ET is primarily sourced from water in the upper few centimetres of unsaturated organic soils (Grewal, Harman, and Carey 2025; Smith et al. 2020), which is largely disconnected from the storage component that directly contributes to discharge. Therefore, as stream chemistry reflects dominant flowpaths, an understanding of typical active layer thaw dynamics across individual thaw seasons could be generated by investigating seasonal thaw with concentration and discharge measurements.

Seasonal and interannual trends in stream chemistry have been used to infer flowpath depth and thaw depth in catchments underlain by permafrost (Barker et al. 2014; Keller et al. 2010;

10991085, 2026, 4, Downloaded from https://onlinelibrary.wiley.com/doi/10.1002/hyp.70512 by Jonathan O'Donnell , Wiley Online Library on [17/09/2026]. See the Terms and Conditions (https://onlinelibrary.wiley.com/terms-and-conditions) on Wiley Online Library for rules of use; OA articles are governed by the applicable Creative Commons License

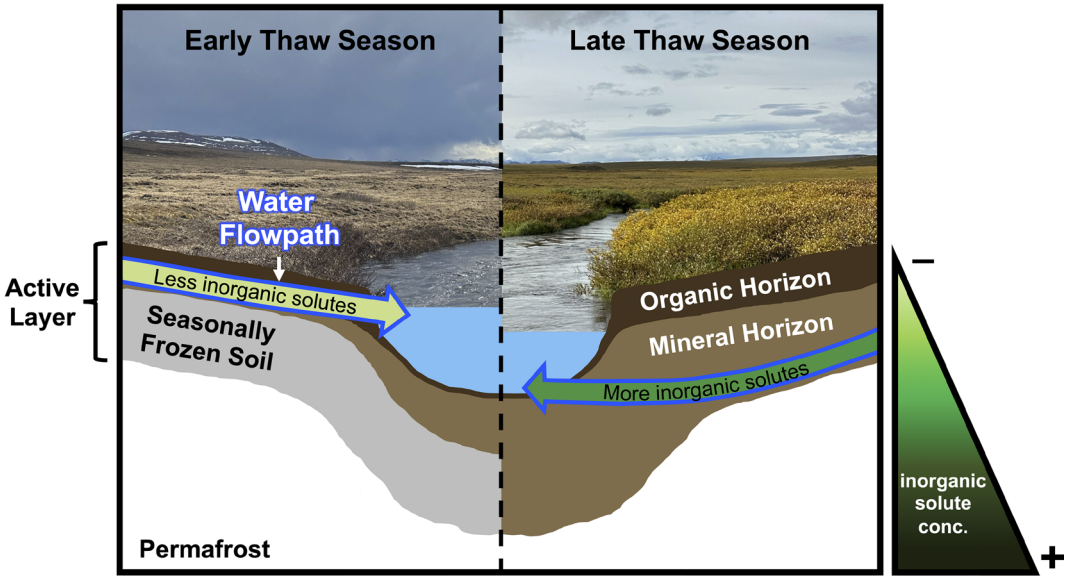


FIGURE 1 | Conceptual diagram showing a cross-section of an Arctic stream and hillslope subsurface in the early thaw season (early June) and the late thaw season (late August) at baseflow conditions. In the early thaw season, much of the active layer is still frozen, restricting water flowpaths to the near-surface soil horizons (i.e., the organic soil horizon and top of the mineral soil horizon), where inorganic solute concentrations are low. In the late thaw season, the active layer is completely thawed and flowpaths are deeper, accessing soil with greater inorganic solute concentrations (i.e., deeper mineral soil horizons).

Lehn et al. 2017; O'Donnell et al. 2014). For example, stream Ca/Na and Ca/Ba ratios increase throughout the thaw season as flowpaths deepen in an Arctic catchment on Alaska's North Slope, suggesting a transition from silicate to carbonate weathering as thaw progresses (Keller et al. 2010). Using streams as sensors to document thaw utilises the following logic: (1) Soil chemistry changes with depth in the soil profile; specifically, some solutes (especially inorganics) increase with depth due to a shift from organic to mineral soils, as well as a shift to more carbonate-rich mineral soils (Figure 1; Keller et al. 2007; Keller et al. 2010); (2) Thaw depth increases throughout the thaw season (i.e., May through September), exposing deeper horizons with more potential for mineral weathering, resulting in increased concentrations of these solutes at depth; and (3) Increased thaw allows water flowpaths to travel more deeply, passing through the deeper soil horizons and carrying greater amounts of the solutes to the stream (Figure 1). While discharge (as a proxy for wetness) can also drive stream solute concentrations by controlling dominant flowpaths, the combined influence of discharge and thaw depth on stream chemistry is rarely disentangled.

In this study, we conducted a detailed assessment of a 'streams as sensors' approach to documenting active layer thaw in three catchments with widely varying environmental characteristics on Alaska's North Slope. We analysed a unique stream chemistry and discharge dataset with generalised additive models (GAMs) to disentangle the effects of discharge and active layer thaw on stream chemistry across three thaw seasons. Specifically, we asked which solutes are sensitive tracers of seasonal ground thaw, and are these tracers consistent across catchments with distinctive landscape characteristics. We hypothesised that relatively conservative solutes such as Ca, Sr and other solutes sourced from mineral weathering would show the significance and model power desired to be used as thaw tracers, as these solutes are abundant, tend to increase in concentration with depth in this region (Keller et al. 2007) and do not undergo major reactions that would change their concentrations during transport to and within the stream channel. However, we also hypothesised that the utility of each tracer would vary between catchment types due to landscape characteristics impacting solute concentrations and reactivity (Tank et al. 2020). The primary goal of this study was to assess the efficacy of solutes as thaw tracers, but through this approach we were also able to identify drivers of solute variability, especially between three contrasting catchments. This study evaluates solutes as tracers of active layer thaw on a seasonal time scale of about 4 months, and does not evaluate solutes as tracers of permafrost thaw and degradation generally occurring on longer timescales (i.e., decades) in which newly thawed permafrost may produce distinct chemical signals compared to soils experiencing repeated seasonal thaw. However, assessing solutes as tracers at a seasonal scale will provide useful insights on the efficacy of solute tracers for detecting permafrost thaw over longer time scales.

2 | Study Site and Methods

2.1 | Study Site

The three study catchments are located near Toolik Field Station on Alaska's North Slope, with their outlet sampling points accessible via the Dalton Highway (Figure 2). The Trevor Creek (hereafter, *Alpine*) catchment is located in the Brooks Range and drains into the Atigun River. Both the Kuparuk River headwaters (*Tundra*) and Oksrukuyik Creek (*Lake-Influenced Tundra*) catchments are located in the northern foothills of the Brooks Range, adjacent to each other but with differing glacial histories. The *Tundra* catchment has been studied for over 40 years and eventually drains directly into the Arctic Ocean. The *Lake-Influenced Tundra* catchment drains into the Sagavanirktok

10991085, 2026, 4, Downloaded from https://onlinelibrary.wiley.com/doi/10.1002/hyp.70512 by Jonathan O'Donnell , Wiley Online Library on [17/09/2026]. See the Terms and Conditions (https://onlinelibrary.wiley.com/terms-and-conditions) on Wiley Online Library for rules of use; OA articles are governed by the applicable Creative Commons License

River. These three catchments span a variety of characteristics common on Alaska's North Slope (Table 1), making this study relevant to other permafrost-underlain catchments.

The study region is underlain by continuous permafrost approximately 150–300 m thick (Osterkamp and Payne 1981) with a maximum active layer thickness of less than 1 m (Cooper

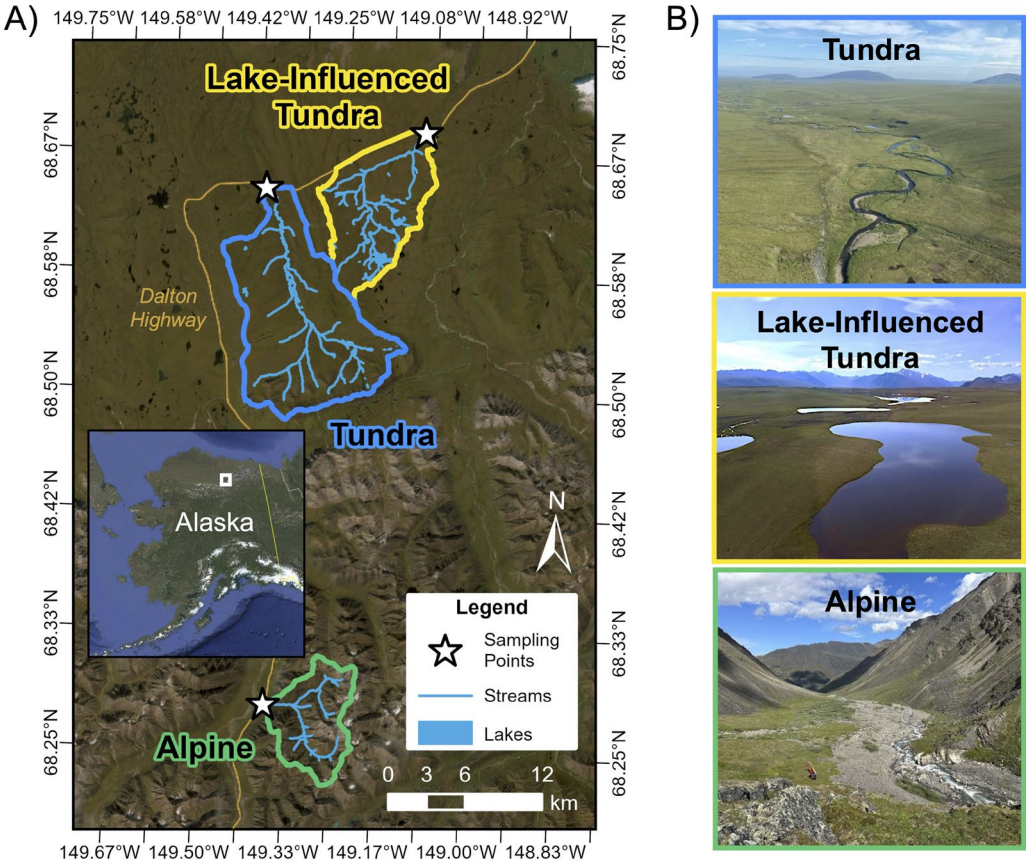


FIGURE 2 | (A) Map of the study catchments. The inset map of Alaska shows the location of these catchments outlined with a white square. The stars indicate the outlets of these catchments where sampling took place. (B) Photographs of the study catchments. The colour scheme for the catchments will continue throughout Section 3.

TABLE 1 | Catchment characteristics for the three study catchments.

	Catchment		
Characteristics	**Tundra**	**Lake-Influenced Tundra**	**Alpine**
River name	Kuparuk River	Oksrukuyik Creek	Trevor Creek
Size (km^2)	134.5	71.7	43.2
Outlet location (°)	68.64313, −149.40326	68.68617, −149.09845	68.28344, −149.37155
Major lithologies	Sandstone, conglomerate, siltstone, shale	Sandstone, conglomerate	Shale, sandstone, conglomerate, limestone
Strahler stream order	4th	3rd	3rd
Average slope (°)	7.1	3.3	29.6
Lake coverage (%)	0.3	3.6	0.0
Tundra type	Wet acidic tundra	Wet acidic tundra	Rocky heath
Tussock tundra coverage (%)	53.2	63.0	0.1
Sparse vegetation coverage (%)	2.3	0.1	8.7
Lichen coverage (%)	0.0	0.0	51.7

10991085, 2026, 4, Downloaded from https://onlinelibrary.wiley.com/doi/10.1002/hyp.70512 by Jonathan O'Donnell , Wiley Online Library on [17/09/2026]. See the Terms and Conditions (https://onlinelibrary.wiley.com/terms-and-conditions) on Wiley Online Library for rules of use; OA articles are governed by the applicable Creative Commons License

et al. 2023; Hinzman et al. 1998; Kane et al. 1991; Nelson et al. 1997; Nyland et al. 2021; Romanowicz and Kling 2022). In terms of major geologic formations, the *Alpine* catchment covers 17% Hunt Fork Shale, 53% Kanayut Conglomerate and Noatak Sandstone, and 20% Kayak Shale (Wilson et al. 2015). The *Tundra* catchment covers 25% Fortress Mountain Formation and 75% unconsolidated surficial deposits, whilst the *Lake-Influenced Tundra* catchment covers 90% unconsolidated surficial deposits (Wilson et al. 2015). The primary lithologies of these units are listed in Table 1 and are dominated by sandstone and conglomerate (Wilson et al. 2015). Between the two low-gradient catchments, the *Tundra* catchment has more exposed and near-surface bedrock, making up 19% of the catchment, whilst the *Lake-Influenced* catchment only has exposed bedrock in about 3% of the catchment (Hamilton 2003). The low-gradient catchments were both recently glaciated by the Sagavanirktok River Glaciation in the middle Pleistocene and the Itkillik Glaciation in the late Pleistocene (between 120 and 50 ka), with 54% of the *Tundra* catchment and 18% of the *Lake-Influenced* catchment impacted by a drift of the Sagavanirktok River Glaciation, and 9% of the *Tundra* catchment and 76% of the *Lake-Influenced* catchment impacted by a drift or outwash of the Itkillik Glaciation (Hamilton 2003).

Other differences between the catchments include a much greater average slope in the *Alpine* catchment (Table 1) and 12 times greater percent lake coverage in the *Lake-Influenced* catchment, which contains over 30 lakes distributed in the headwater tributaries (Wilson et al. 2015). Whilst the valleys of the *Alpine* catchment are vegetated and contain thin to no organic soils (Lehn et al. 2017), the two low-gradient tundra catchments have thicker peaty organic soils (20–40 cm in thickness; Walker and Walker 1996) and much greater vegetation coverage, dominated by tussock tundra (Table 1; Jorgenson et al. 2009). Cottongrass (*Eriophorum vaginatum*) makes up much of the ground cover here, with dwarf shrubs including birch (*Betula nana*) and willow (*Salix* spp.) appearing in the riparian areas (Huryn and Hobbie 2012). Meanwhile, the *Alpine* catchment is dominated by lichen, which covers 51.7% of the catchment (Jorgenson et al. 2009).

2.2 | Direct Thaw Depth Measurements

For the 2022 and 2023 summer thaw seasons (May through September), we measured thaw depth weekly via depth-to-resistance probing (*sensu* Brown et al. 2000) at transects adjacent to the stream outlet. Each transect consisted of eight sites perpendicular to the stream from 3 to 24 m away from the channel, spaced 3 m apart. We were unable to obtain reliable thaw depth measurements via probing in the *Alpine* catchment due to the rocky subsurface. We compared our values to reported values in the region to confirm the validity of our measurements (Kling 2025; Shiklomanov 2025).

2.3 | Discharge

Across the 2021–2023 thaw seasons, we measured discharge at the catchment outlets by recording continuous stage with HOBO U20 Water Level Data Loggers (Onset HOBO, Bourne, Massachusetts, USA) and making instantaneous discharge measurements via salt injections whilst measuring conductivity with HOBO U24 Conductivity Loggers (Onset HOBO, Bourne, Massachusetts, USA), or using a SonTek FlowTracker (YSI Inc., Yellow Springs, Ohio, USA). We calculated stage–discharge relationships for each stream in each year to create continuous discharge records throughout the thaw seasons. We excluded the freshet period at the beginning of the thaw season in this analysis as accurate measurements of discharge were not possible due to bed ice and bank overflow conditions. The end of the freshet period was determined via daily photographs of the channel outlets, where we looked for a decline in the bulk of channel ice, bed ice, bank ice and snowpack. In 2021 and 2023, the continuous measurement of discharge in the *Tundra* and *Lake-Influenced Tundra* catchments did not begin until about a week after the freshet period ended. We do not have discharge measurements in the *Alpine* catchment for 2021 due to a sensor malfunction. Also in the *Alpine* catchment, we only have point measurements from each water chemistry sampling date for the first half of the 2023 thaw season due to flooding destroying the staff gauge and water level logger.

2.4 | Water Chemistry Sample Collection

During the 2021–2023 thaw seasons, we collected ~weekly samples at the outlets of the three study catchments where the Dalton Highway provides access to the streams (Figure 2; Table 1). We collected grab samples in amber HDPE Nalgene bottles, rinsing each bottle thrice with stream water before collecting the sample by submerging the bottle in the stream. As the Dalton Highway is periodically treated with calcium carbonate and generates dust that can be deposited on the adjacent tundra (Ackerman and Finlay 2019; Walker and Everett 1987), we completed our sampling > 100 m upstream of the road crossing to limit road dust influence on the samples.

2.5 | Laboratory Analysis

We syringe-filtered all stream samples through 0.2 μm cellulose acetate filters (Sartorius 1110725N) within 8 h of collection into triple-rinsed amber HDPE bottles and refrigerated them until shipping in coolers to Brigham Young University for sample analysis. There, we refrigerated the samples until analysis for total amounts of geogenic elements (Al, As, B, Ba, Br, Ca, Cd, Co, Cr, Cu, Fe, K, Mo, Mg, Mn, Na, Ni, P, Pb, S, Se, Si, Sn, Sr, Ti, V, Zn) on an inductively coupled plasma mass spectrometer (ICP-MS, iCAP 7000 series, Thermo Scientific). We analysed these specific geogenic elements as many of them are conservative along flowpaths and have been shown to change with depth in the soil profile in the study region (Barker et al. 2014; Keller et al. 2007; Lehn et al. 2017), making them suitable candidates for tracers of ground thaw. The ICP-MS had a detection limit of 0.02 mg L^{-1} and only Ba, Ca, Fe, K, Na, Mg, S, Si and Sr were above detection in most samples. For this analysis, we reported concentrations of these nine elements that fell below the detection limit as half the detection limit (Reimann et al. 2008; Shogren et al. 2022). We did not report Fe in the *Alpine* catchment as nearly 90% of samples measured were below the detection limit.

10991085, 2026, 4, Downloaded from https://onlinelibrary.wiley.com/doi/10.1002/hyp.70512 by Jonathan O'Donnell , Wiley Online Library on [17/09/2026]. See the Terms and Conditions (https://onlinelibrary.wiley.com/terms-and-conditions) on Wiley Online Library for rules of use; OA articles are governed by the applicable Creative Commons License

2.6 | Data Analysis

We used GAMs (S. N. Wood 2017) to extend the classic C–Q model by adding a spline seasonality term which accounted for a non-linear relationship between concentration and Day of Year (DOY; Grewal, Nicholls, and Carey 2025):

$$\log(C) = b \times \log(Q) + \log(a) + \text{sDOY} \quad (1)$$

where C is the concentration of the solute, b and a are constant coefficients, Q is the discharge, and sDOY is the spline term which varies based on the day of year.

We combined the 3 years of data for each catchment (only 2 years for the *Alpine* catchment due to missing 2021 discharge data) and used GAMs to determine the impact of discharge and seasonality on concentration using the *mgcv* package in R (S. Wood 2020). The smooth function for seasonality (sDOY) was specified using a thin plate regression spline, the default smoother in *mgcv*. Model complexity was constrained through penalisation, with smoothing parameters estimated using restricted maximum likelihood (REML) and a default penalty inflation factor ($\gamma = 1$) such that the effective degrees of freedom (edf) of sDOY were determined by the data rather than fixed knot placement. Model residuals were evaluated for normality via visual inspection of Q–Q plots for each solute and catchment. Log–log C–Q slopes extracted from GAMs identify whether the solute behaviour may be defined as dilution or flushing (Godsey et al. 2009), potentially reflecting heterogeneity of soil chemistry (Stewart et al. 2022; Zhi et al. 2019). The sDOY term reflects the influence of seasonality on the C–Q model. Since the term is logarithmic, a change of one represents a factor of 10 change in concentration if discharge is held constant. The standard error reported by GAMs captures interannual variability in seasonality that may occur when combining multiple years of data.

For models with significant p-values for sDOY ($p < 0.1$), we show the partial effect plots of the sDOY term with standard error, which varies with DOY. For each solute in each catchment, we report log–log C–Q slope with standard error and p-value, sDOY range with mean standard error and p-value, and model R^2. In the context of GAMs, we defined a solute as an effective tracer of thaw if it had a significant C–Q slope ($p < 0.1$), a significant sDOY term ($p < 0.1$) and a relatively high model R^2 (> 0.4). Strong C–Q slopes can reflect vertical chemical gradients in soils (high flows reflecting high water tables and shallow flowpaths, and low flows reflecting lower water tables and deep flowpaths; Stewart et al. 2022; Zhi et al. 2019), horizontal variation in chemical stores in soils and heterogeneity across a catchment (Godsey et al. 2009), and/or differences in solubility (Moatar et al. 2017). Insignificant C–Q slopes indicate homogeneous vertical and lateral chemical gradients within the soil profile, a thermodynamic limit which is quickly reached (Maher and Chamberlain 2014), and/or dominance of instream reach-scale biogeochemical processes (Godsey et al. 2009). A significant sDOY term reflects seasonal changes in chemistry driven by processes other than discharge. Together, significant sDOY terms and C–Q slopes indicate changes in concentration due to thaw, as sDOY indicates there are changes in chemistry across the thaw season during which thaw depth increases, and C–Q slope shows a concentration gradient and stream chemistry driven by variability in discharge (i.e., depth of flowpath according to the 'shallow and deep hypothesis'; Stewart et al. 2022; Zhi et al. 2019). Whilst a significant C–Q slope can also indicate horizontal variation in soil chemistry or differences in solubility by itself, when the sDOY term is significant, it indicates changes in chemistry due to seasonal processes (i.e., thaw). A significant sDOY term with an insignificant C–Q slope indicates that seasonal processes other than thaw are impacting concentrations (Grewal, Nicholls, and Carey 2025), as an insignificant C–Q slope indicates homogeneity in solute sources across soil depths, or that changing flowpaths do not strongly impact stream chemistry. Finally, the model R^2 (which is adjusted based on the edf) represents the explanatory power of discharge and seasonality on stream chemistry. By using GAMs to account for both the impacts of discharge and seasonality on concentration, we were able to use all of the stream chemistry and discharge data collected rather than omit data over a certain discharge threshold as done in previous studies examining tracers of thaw (Keller et al. 2010; Lehn et al. 2017), and account for discharge effects on solute dilution and enrichment.

3 | Results

3.1 | Thaw Depth

Depth-to-resistance probing revealed increases in thaw depth in both the *Tundra* and *Lake-Influenced Tundra* catchments across the 2022 and 2023 thaw seasons (Figure 3). At the end of the sampling period in 2022, thaw depth in the *Lake-Influenced* catchment was 13 cm greater than the *Tundra* catchment, whilst both catchments thawed to about the same depth in 2023. The values were within the range

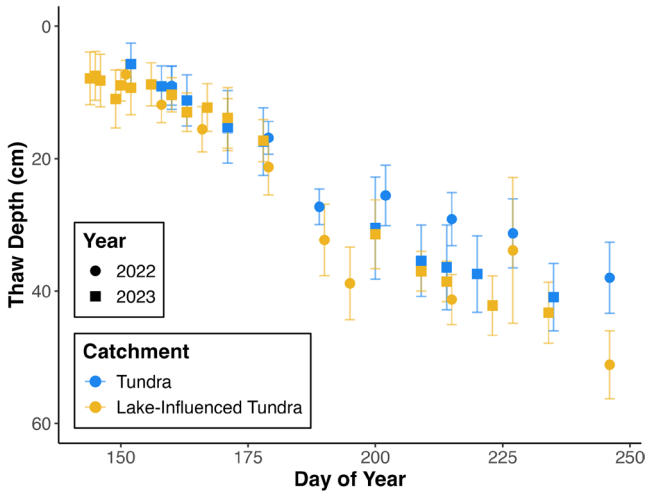


FIGURE 3 | Thaw depth throughout the 2022 and 2023 thaw seasons for the *Tundra* and *Lake-Influenced Tundra* catchments, measured via depth-to-resistance probing of 8 sites along a 24 m transect perpendicular to the stream. Each point represents the average of these measurements for a specific sampling date, with the error bars showing standard deviation.

10991085, 2026, 4, Downloaded from https://onlinelibrary.wiley.com/doi/10.1002/hyp.70512 by Jonathan O'Donnell , Wiley Online Library on [17/09/2026]. See the Terms and Conditions (https://onlinelibrary.wiley.com/terms-and-conditions) on Wiley Online Library for rules of use; OA articles are governed by the applicable Creative Commons License

of nearby measurements of thaw depth carried out by the Arctic Long Term Ecological Research (LTER) Station and the Circumpolar Active Layer Monitoring (CALM) Network (Kling 2025; Shiklomanov 2025).

3.2 | Discharge

The mean and median flows increased in each catchment across the 3-year period (Table 2). The *Lake-Influenced Tundra* catchment had the smallest discharge of the three rivers, whilst the *Alpine* and *Tundra* catchments had similar flows. Water chemistry sampling events included multiple high flow events and spanned 86%, 73%, and 50% of the total observed flow range for the *Tundra*, *Lake-Influenced Tundra* and *Alpine* rivers respectively, excluding the largest flood event in 2023 where we did not have reliable discharge data (Figure 4).

3.3 | Water Chemistry

There were a few common patterns in solute concentrations between the three catchments; quantitative summaries of concentrations separated by catchment are provided in Table S1. For Ca, K, Mg and S, the *Tundra* and *Lake-Influenced Tundra* catchments had similar ranges and values, whilst the *Alpine* catchment had greater concentrations (Figure 5). The *Alpine* and *Lake-Influenced Tundra* catchments had similar concentrations for Ba and Si, whilst the *Tundra* catchment had greater concentrations. For Na and Sr, the *Lake-Influenced Tundra* catchment had the smallest concentrations, whilst the *Tundra* catchment had slightly greater concentrations and the *Alpine* catchment had the largest concentrations. These inter-catchment patterns persisted from year to year, although the concentration values shifted.

For Ca, K, Mg, Na, S, and Sr, the greatest maximum concentration occurred in the *Alpine* catchment in the late thaw season of 2021 (Figure 5). These concentrations were often more than twice the maximum concentrations in other years. The smallest observed concentrations often occurred in the early thaw season in the *Lake-Influenced Tundra* catchment and were near or at the instrument detection limit of 0.02 mg L^{-1}.

3.4 | GAMs

GAMs results showed significant seasonality ($p < 0.1$) for five solutes in the *Alpine* catchment (Ca, Mg, Na, S, Sr), seven solutes in the *Lake-Influenced Tundra* catchment (Ba, Ca, Fe, Mg, Na, Si, Sr) and four solutes in the *Tundra* catchment (Ba, Ca, K, Si; Figure 6). Model residuals were generally normally distributed except for K in the *Lake-Influenced Tundra* catchment. The sDOY term was linear (edf = 1.0) and increasing with day of year in the *Alpine* catchment for all solutes with significant seasonality ($p < 0.1$; Figure 6). In the *Tundra* catchment, the sDOY for K was linear (edf = 1.0) and decreasing, whilst all other significant solutes were non-linear (edf > 2.2), increasing at the beginning of the thaw season and decreasing later in the season (Figure 6). For the *Lake-Influenced Tundra* catchment, the significant sDOY terms were linear

TABLE 2 | Summary of discharge (L s^{-1}) for each thaw season in each catchment.

	Catchment											
	Tundra				Lake-Influenced Tundra				Alpine			
Year	Dates monitored	Mean	Median	Range	Dates monitored	Mean	Median	Range	Dates monitored	Mean	Median	Range
2021	6/20/21–8/23/21	1976	1318	415–8675	6/17/21–9/23/21	859	558	213–5117	—	—	—	—
2022	6/9/22–9/3/22	2135	1744	822–8980	6/8/22–8/30/22	1472	835	362–10871	6/4/22–9/2/22	2202	2057	226–12810
2023	6/17/23–9/4/23[a]	3023	2010	607–10787	6/17/23–9/4/23[a]	1648	1242	327–7151	7/25/23–9/2/23	4393	4267	2447–8464

[a]In 2023, we were unable to get reliable discharge measurements from the afternoon of July 8 to the morning of July 10 due to a large storm resulting in discharge much beyond the rating curve limits. Therefore, the summary statistics for the *Tundra* and *Lake-Influenced Tundra* catchments in 2023 are likely underestimates.

10991085, 2026, 4, Downloaded from https://onlinelibrary.wiley.com/doi/10.1002/hyp.70512 by Jonathan O'Donnell , Wiley Online Library on [17/09/2026]. See the Terms and Conditions (https://onlinelibrary.wiley.com/terms-and-conditions) on Wiley Online Library for rules of use; OA articles are governed by the applicable Creative Commons License

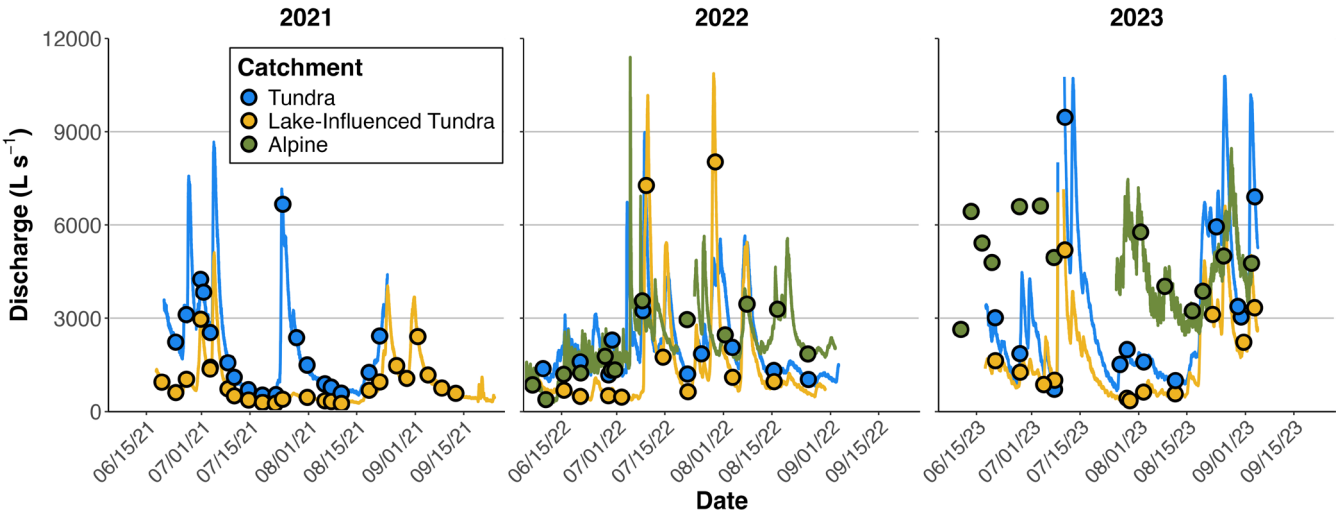


FIGURE 4 | Discharge across the thaw seasons for 2021–2023, with circles showing dates and points on the hydrograph when water chemistry grab samples were collected. Discharge in the *Alpine* catchment was unavailable for 2021 and part of 2023, for reasons detailed in Section 2. Discharge in both the *Tundra* and *Lake-Influenced Tundra* catchments was unavailable briefly during a large storm from the afternoon of 8 July 2023 to the morning of 10 July 2023.

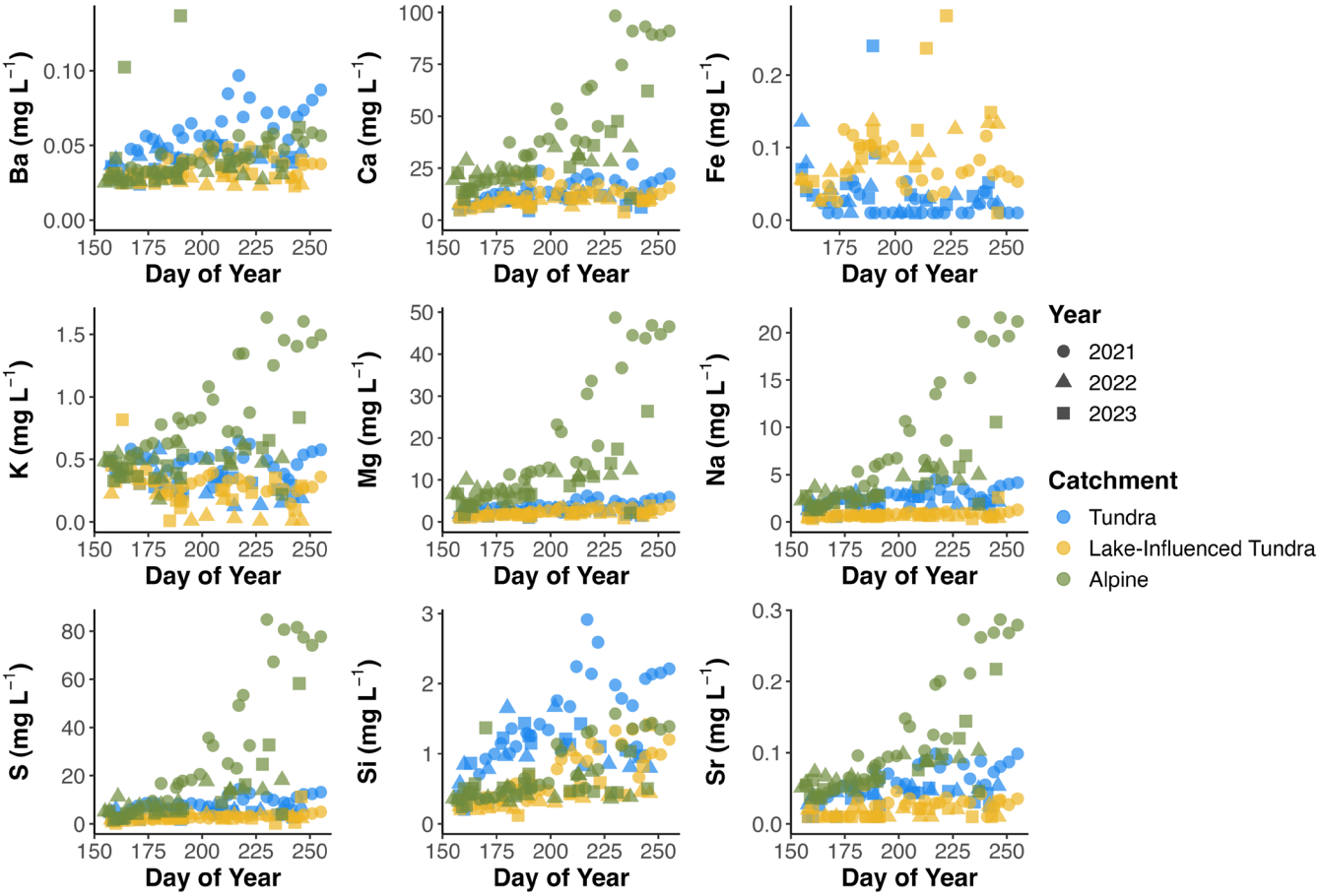


FIGURE 5 | Solute concentrations across each thaw season. Fe was often below the detection limit in the *Alpine* catchment and therefore is not included here. The greatest overall concentration for many solutes occurred in the 2021 late thaw season.

and increasing for Ba and Mg (edf = 1.0), nearly linear and increasing for Na, Si and Sr (1.1 < edf < 1.7) and non-linear for Ca and Fe (edf > 2.7).

The largest sDOY range, indicating the greatest change in concentration due to seasonality, was for S in the *Alpine* catchment (sDOY range = 0.94; Table 3). The smallest yet still significant

10991085, 2026, 4, Downloaded from https://onlinelibrary.wiley.com/doi/10.1002/hyp.70512 by Jonathan O'Donnell , Wiley Online Library on [17/09/2026]. See the Terms and Conditions (https://onlinelibrary.wiley.com/terms-and-conditions) on Wiley Online Library for rules of use; OA articles are governed by the applicable Creative Commons License

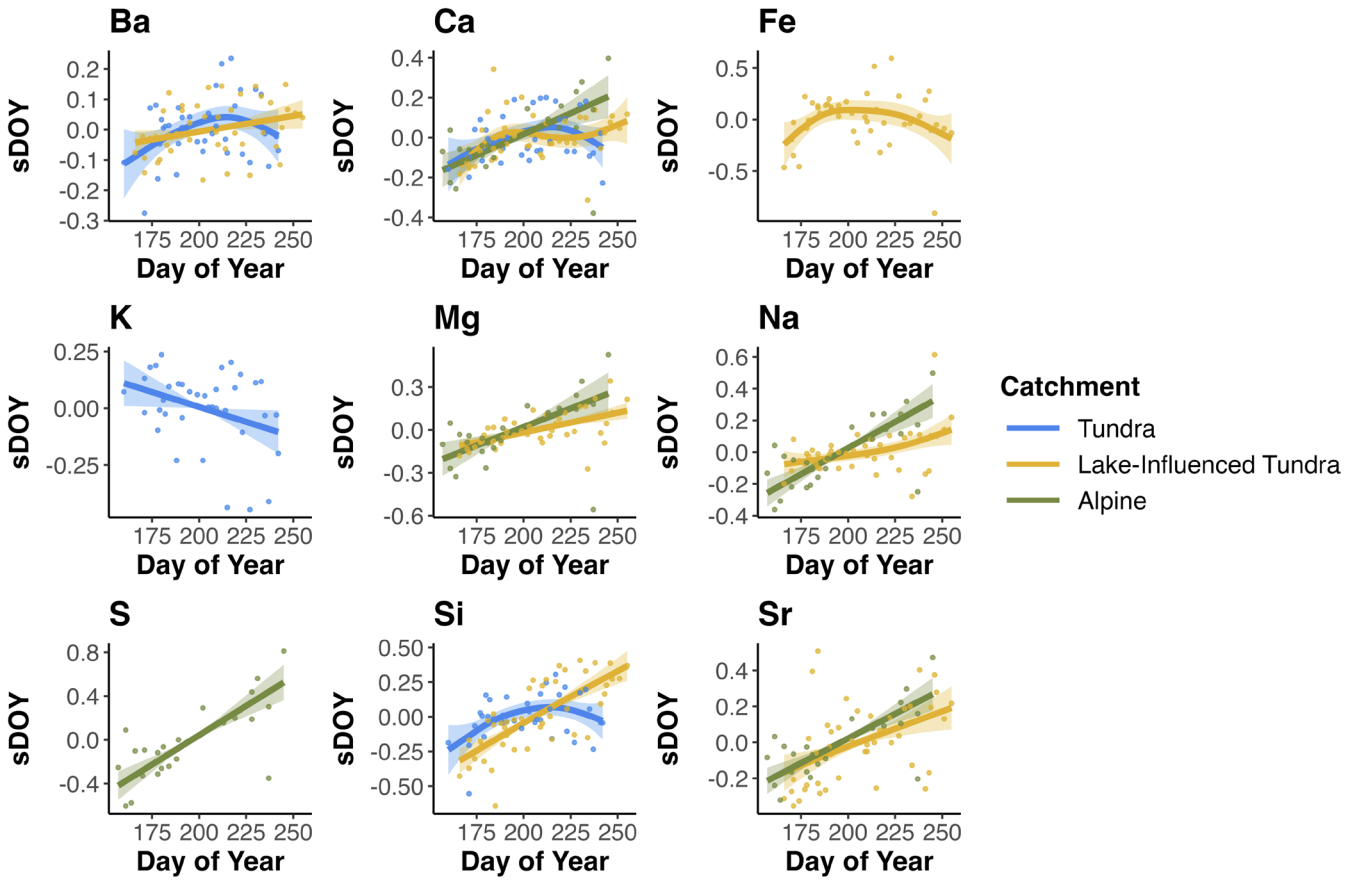


FIGURE 6 | Partial effect plots of the sDOY term across the thaw season, only shown when sDOY is significant ($p < 0.1$). Standard error is shown with shading and changes in magnitude throughout the thaw season. Residuals are plotted as points. The sDOY term indicates the change in concentration that can be attributed to seasonality. For example, in the *Alpine* catchment, if discharge is held constant, there is an increase of about 0.94 in the sDOY for S across the thaw season. As sDOY is $\log_{10}$, this represents an 8.7-fold increase in concentration.

sDOY range was for Ba in the *Lake-Influenced Tundra* catchment (sDOY range = 0.09). Si in the *Lake-Influenced Tundra* catchment had the second largest sDOY range (0.68), and Si also showed the greatest seasonality of all solutes in the *Tundra* catchment (sDOY range = 0.31, 9th greatest seasonality overall). The *Alpine* catchment had five of the top six solutes exhibiting the greatest seasonality (in order of largest to smallest sDOY range: S, Na, Sr, Mg, Ca; Figure 7; Table 3).

The greatest positive log–log *C*–*Q* slope was for Fe in the *Tundra* catchment (slope = 0.58; Figure 7; Table 3), followed by Ba and Si in the *Alpine* catchment (slope = 0.22 and 0.18 respectively) and Fe and Si in the *Lake-Influenced Tundra* catchment (slope = 0.11 and 0.04 respectively). All other log–log *C*–*Q* slopes were negative, indicating diluting effects. The strongest negative slope was for S in the *Alpine* catchment (slope = −0.40), followed by S in the *Tundra* catchment (slope = −0.33) and Sr in the *Lake-Influenced Tundra* catchment (slope = −0.30). For *C*–*Q* slopes near zero (e.g., Ba in the *Lake-Influenced Tundra* catchment), the CV ratio can be used to determine whether a solute is chemostatic (small CV ratio) or chemodynamic (large CV ratio), irrespective of the *C*–*Q* slope (Table 3). All of the solutes with *C*–*Q* slopes near zero (±0.20) had CV ratios greater than 0.50, indicating they were chemodynamic (Godsey et al. 2009; Li et al. 2017).

Seven models had R^2 values greater than 0.4, including Ca in the *Tundra* catchment, Ca, Mg and Si in the *Lake-Influenced Tundra* catchment, and S, Na and Sr in the *Alpine* catchment (Table 3). The R^2 values for K were less than 0.2 in all catchments, including the smallest R^2 value overall of 0.03 for K in the *Alpine* catchment.

4 | Discussion

The rate of release of permafrost carbon and nutrients depends in part on how lateral water fluxes interact with soils. However, the logistical challenges associated with measuring ground thaw (a major control of hydrological routing and consequently lateral flux) at large scales and with high temporal resolution highlight the need for new, more practical approaches to detect thaw, especially at spatiotemporal scales greater than achieved with point measurements. In this study, we found that stream chemistry measurements and GAMs hold promise for quantifying catchment-scale ground thaw processes. We also found that there was no single effective geochemical tracer of thaw for the different landscapes studied; however, our methods could easily be used to rate the value of different solutes as thaw tracers.

10991085, 2026, 4, Downloaded from https://onlinelibrary.wiley.com/doi/10.1002/hyp.70512 by Jonathan O'Donnell , Wiley Online Library on [17/09/2026]. See the Terms and Conditions (https://onlinelibrary.wiley.com/terms-and-conditions) on Wiley Online Library for rules of use; OA articles are governed by the applicable Creative Commons License

TABLE 3 | GAMs output for each catchment and solute.

Catchment	Solute	*C–Q* slope	*C–Q* slope standard error	*C–Q* slope *p*-value	CV ratio	sDOY range	sDOY mean standard error	sDOY *p*-value	Model R^2
Tundra	Ba	−0.15	0.06	0.01*	2.71	0.15	0.05	0.10*	0.30
	Ca	−0.22	0.06	0.00*	0.74	0.19	0.06	0.08*	0.41
	Fe	0.58	0.14	0.00*	15.05	0.30	0.11	0.24	0.39
	K	−0.22	0.09	0.02*	1.86	0.22	0.05	0.03*	0.17
	Mg	−0.28	0.07	0.00*	0.99	0.09	0.05	0.43	0.36
	Na	−0.27	0.07	0.00*	1.08	0.17	0.06	0.16	0.37
	S	−0.33	0.09	0.00*	1.10	0.05	0.05	0.61	0.25
	Si	−0.18	0.08	0.04*	1.35	0.31	0.08	0.03*	0.31
	Sr	−0.28	0.08	0.00*	4.27	0.23	0.07	0.11	0.36
Lake-Influenced Tundra	Ba	−0.11	0.03	0.00*	2.44	0.09	0.02	0.04*	0.21
	Ca	−0.24	0.04	0.00*	0.62	0.23	0.06	0.05*	0.46
	Fe	0.11	0.10	0.28	3.90	0.33	0.12	0.08*	0.14
	K	−0.27	0.16	0.11	4.17	0.27	0.16	0.36	0.06
	Mg	−0.20	0.04	0.00*	0.77	0.25	0.03	0.00*	0.50
	Na	−0.13	0.05	0.01*	1.00	0.22	0.05	0.01*	0.24
	S	−0.16	0.09	0.07*	1.24	0.14	0.06	0.22	0.06
	Si	0.04	0.07	0.59	2.00	0.68	0.05	0.00*	0.56
	Sr	−0.30	0.08	0.00*	11.54	0.36	0.06	0.00*	0.34
Alpine	Ba	0.22	0.09	0.02*	4.58	0.17	0.07	0.19	0.28
	Ca	−0.18	0.10	0.09*	0.87	0.37	0.05	0.00*	0.35
	K	−0.07	0.10	0.49	1.50	0.16	0.05	0.11	0.03
	Mg	−0.25	0.14	0.08*	1.36	0.46	0.07	0.00*	0.30
	Na	−0.23	0.10	0.03	1.49	0.58	0.05	0.00*	0.59
	S	−0.40	0.15	0.01*	2.02	0.94	0.07	0.00*	0.62
	Si	0.18	0.11	0.10*	1.63	0.04	0.05	0.73	0.09
	Sr	−0.17	0.08	0.06*	3.68	0.48	0.04	0.00*	0.58

Note: C–Q slope represents the fitted linear coefficient between $\log_{10}$-transformed concentration and $\log_{10}$-transformed discharge; negative slopes indicate dilution with increasing discharge, whilst positive slopes indicate enrichment. *C–Q* slope standard error is the standard error of the fitted discharge coefficient, and *C–Q* slope *p*-value is the significance of the slope ($p < 0.1$; significant values denoted by *). Values reported as $p = 0.10$ but marked significant correspond to $p = 0.099$ prior to rounding. The CV ratio is the ratio of the coefficient of variance for concentration and discharge (CV_C/CV_Q), which quantifies the variability of solute concentrations relative to discharge variability. Small CV ratios indicate more chemostatic behaviour, whilst larger values indicate more chemodynamic behaviour. The sDOY range represents the range of the fitted seasonal smooth term, expressed in $\log_{10}$ units, meaning a value of 1 indicates a 10-fold seasonal change in concentration. The sDOY mean standard error is the mean standard error of the fitted seasonal smooth term, and the sDOY *p*-value is the significance of the seasonal smooth term. Finally, the model R^2 shows the predictive power of the model, with $R^2 > 0.4$ indicating relatively strong model performance.

4.1 | Identified Effective Tracers of Ground Thaw in the Study Catchments

Several solutes were abundant in stream water and had both significant log–log *C–Q* slopes and significant seasonality (sDOY) terms, making them possible effective tracers of thaw. However, model performance varied between the catchments. Solutes with significant *C–Q* slopes ($p < 0.1$), significant seasonality ($p < 0.1$) and the greatest R^2 values (> 0.4) were deemed effective tracers. The solutes that met these tracer criteria were primarily mineral weathering products as we hypothesised; however, not all mineral weathering products met the tracer criteria. Additionally, as hypothesised, the solutes that met the criteria varied between catchments, likely due to differences in catchment characteristics, which are explored in Section 4.2. The solutes that met the tracer criteria

10991085, 2026, 4, Downloaded from https://onlinelibrary.wiley.com/doi/10.1002/hyp.70512 by Jonathan O'Donnell , Wiley Online Library on [17/09/2026]. See the Terms and Conditions (https://onlinelibrary.wiley.com/terms-and-conditions) on Wiley Online Library for rules of use; OA articles are governed by the applicable Creative Commons License

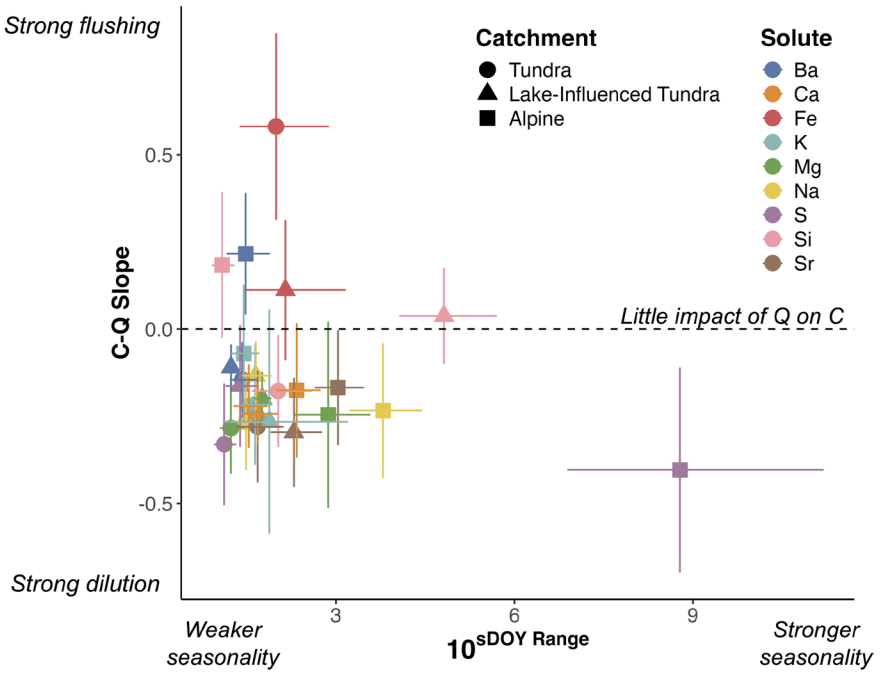


FIGURE 7 | The log–log *C*–*Q* slope versus $10^{\text{sDOY Range}}$ for all solutes. As sDOY Range is $\log_{10}$, here we show $10^{\text{sDOY Range}}$, or the factor by which the concentration changes based only on seasonality. The value represents the magnitude of increase or decrease in concentration if discharge is held constant (i.e., a value of 6 indicates a 6-fold increase or decrease). Horizontal error bars indicate uncertainty in the $10^{\text{sDOY Range}}$ (±1 standard error). For the *C*–*Q* slope, a value near zero (dotted line) indicates little impact of discharge on the solute concentration. A value closer to 1 indicates a flushing effect, as concentration increases with increasing discharge, whilst a value closer to −1 indicates a diluting effect, as concentration decreases with increasing discharge. Vertical error bars show 95% confidence intervals for the *C*–*Q* slopes. An effective tracer of ground thaw will show strong seasonality and a *C*–*Q* slope indicating a strong diluting or flushing effect.

included Ca in the *Tundra* catchment, Ca and Mg in the *Lake-Influenced Tundra* catchment, and Na, S, and Sr in the *Alpine* catchment.

Solutes that showed significance for only *C*–*Q* or only seasonality may be indicators of catchment dynamics but not necessarily thaw conditions. For example, significance for only *C*–*Q* (e.g., S in the *Tundra* catchment) could indicate differences in solute concentrations with distance from the stream rather than depth in the subsurface, as areas farther from the stream are activated during high flows (Godsey et al. 2009; Hewlett and Hibbert 1967). On the other hand, significance for seasonality but not *C*–*Q* (e.g., Si in the *Lake-Influenced Tundra* catchment) could indicate that other seasonal processes besides thaw influence seasonality in stream solute concentrations, for example plant uptake and senescence. If the solute is not impacted by either *C*–*Q* or seasonality, or if the model R^2 is poor, there are likely processes besides discharge and seasonality that strongly impact how these solutes act, such as biogeochemical reactions within or near the stream including in-channel or hyporheic removal or addition processes (Bowden et al. 2008; Zarnetske et al. 2012).

C–*Q* relationships were significant ($p < 0.1$) for all nine solutes in the *Tundra* catchment, six solutes in the *Lake-Influenced Tundra* catchment and all solutes except K in the *Alpine* catchment, likely reflecting heterogeneity in solute concentrations within the subsurface (Table 3). Most *C*–*Q* slopes were negative, indicating increasing soil solute concentrations with depth based on the 'shallow and deep hypothesis', or a lack of near-stream solute pools compared to farther up the hillslope (Figure 7; Table 3; Godsey et al. 2009; Shogren et al. 2021; Stewart et al. 2022; Zhi and Li 2020; Zhi et al. 2019). These results are consistent with prior studies in catchments spanning sporadic to continuous permafrost in Alaska and northern Canada, where Ca, Mg and Na typically show a negative relationship with discharge (Carey et al. 2013; Grewal, Nicholls, and Carey 2025; MacLean et al. 1999; Petrone et al. 2006). Skierszkan, Carey, et al. (2024) found that Fe had positive *C*–*Q* slopes in multiple discontinuous permafrost catchments in subarctic Canada, consistent with our findings. We found considerable variability in Si *C*–*Q* slopes across catchments, with a significant negative slope, a significant positive slope and an insignificant slope in the *Tundra*, *Alpine* and *Lake-Influenced Tundra* catchments respectively (Table 3). In contrast, MacLean et al. (1999) found consistent significant positive Si *C*–*Q* slopes in two catchments in the discontinuous permafrost region of Alaska. The variability in *C*–*Q* slopes between catchments highlights the variation in Si dynamics which may be attributable to differences in catchment characteristics, in particular soil and underlying geology (Beusen et al. 2009; Davis 1964). Additionally, deeper maximum thaw late in the thaw season may allow flowpaths to access previously perennially frozen stores of solutes, resulting in a large flux of solutes to the stream and potentially impacting *C*–*Q* relationships for multiple different solutes.

Significance in the seasonality term of GAMs was less frequent than in *C*–*Q* slopes, with 16 out of 26 of the models showing significant seasonality ($p < 0.1$). Across permafrost catchments in general, Ca and Mg concentrations in streams tend to increase

10991085, 2026, 4, Downloaded from https://onlinelibrary.wiley.com/doi/10.1002/hyp.70512 by Jonathan O'Donnell , Wiley Online Library on [17/09/2026]. See the Terms and Conditions (https://onlinelibrary.wiley.com/terms-and-conditions) on Wiley Online Library for rules of use; OA articles are governed by the applicable Creative Commons License

from spring to fall, reflecting increased thaw of the deeper, mineral soil horizons (Gödde et al. 2024; Grewal, Nicholls, and Carey 2025; Lehn et al. 2017). This pattern is evident both in our study catchments and in other Arctic regions, including Northwestern Canada and Svalbard (Gödde et al. 2024; Grewal, Nicholls, and Carey 2025). For example, in a comparison of catchments underlain by sporadic to continuous permafrost, Grewal, Nicholls, and Carey (2025) found the greatest Ca and Mg seasonality in continuous permafrost sites, consistent with our results. Similarly, Cornwell (1992) found that chemical weathering supplied over 85% of the exported Ca and Mg in the *Tundra* catchment, with exports peaking when thaw depth was greatest. This supports the use of Ca and Mg as tracers, as they are direct products of weathering that are mobilised following ground thaw. Na shows a less consistent seasonal signal across studies. Lehn et al. (2017) observed increasing Na over the thaw season in the study region, whereas Cornwell (1992) reported that precipitation-derived Na could account for up to half of the export, potentially masking hillslope thaw signals. However, we expect that Na is not primarily a signal of precipitation in this study, as Na showed significant negative *C*–*Q* relationships and we would expect precipitation-sourced Na to result in positive or insignificant relationships. Everett et al. (1989) found decreases in Na and Si in hillslope water over time, though their minimal sampling regime (three times between July and August) limits comparison. Si showed significant seasonality in our study, and Carey et al. (2020) also found increasing Si with expanding active layer thickness across a north–south transect in Alaska. For Ba, we did not detect significant seasonality in the *Alpine* catchment, but Barker et al. (2014) reported late-season Ba increases in a nearby mountain catchment. However, their analysis did not consider discharge effects, which may dilute or flush Ba. Barker et al. (2014) likewise found that Fe increased late in the season in a subcatchment of the *Tundra* catchment, but we did not see a significant increase in our analysis. Given the much smaller size of the subcatchment in their study (2.2 km^2 vs. our 134.5 km^2), Fe signals from the hillslopes may have been preserved over shorter transport distances. Supporting this, Everett et al. (1989) found late-season Fe peaks in direct samples of subsurface hillslope water from the same subcatchment. At our larger study scale, Fe may undergo reactions such as photoreduction in the stream before reaching our sampling point (McKnight et al. 1988).

The solutes that met the tracer criteria (i.e., strong model R^2 and significant *C*–*Q* relationship and seasonality) are related in that they are common weathering products in the North Slope region and are generally more conservative along flowpaths both in-stream and in the hillslope compared to other solutes (e.g., Fe). The catchment geology includes sandstone and conglomerate, with the *Alpine* catchment also including limestone. Some of the major weathering elements of these rock types include Ca, Si and Mg, with shale in the *Tundra* and *Alpine* catchments also producing K, Na and S (Wilson et al. 2015). Additionally, studies extracting soil cores have found a switch from silicate to carbonate weathering with depth in this region, producing more Ca at greater depths (Keller et al. 2007; Keller et al. 2010). In the *Tundra* and *Alpine* catchments, Lehn et al. (2017) found that carbonate weathering by carbonic and sulphuric acids as well as silicate weathering by carbonic acids dominated, likely producing Ca and Sr. Nearby the study area, Mg and S were found to increase with depth in the soil (Keller et al. 2007) and we found evidence of this in significant ($p < 0.1$) *C*–*Q* relationships showing dilution behaviour in the study catchments (i.e., at higher flows, shallower flowpaths are activated which flow through soil horizons with less Mg and S). Solutes that are more reactive did not meet tracer criteria often. For instance, K was the only solute that did not have a significant *C*–*Q* slope or sDOY, in both the *Alpine* and *Lake-Influenced Tundra* catchments. In the *Tundra* catchment, even though K had significant *p*-values for *C*–*Q* slope and sDOY, it did not meet the criteria for an effective tracer due to a very poor model R^2, meaning this element is likely influenced by factors other than discharge and seasonality. Fe, which also did not qualify as an effective tracer, is highly redox-sensitive and readily oxidised and reduced by microbes in the extensive oxic–anoxic interfaces present in water-logged tundra soils (Emerson et al. 2015; Michaud et al. 2023). There is also evidence that dissolved Fe moves upward from mineral to organic soils and precipitates as Fe oxides at the redox interface, suggesting that Fe may not follow a simple vertical soil concentration gradient across the study catchments (Herndon et al. 2017).

4.2 | Using Stream Solutes as Ground Thaw Tracers Requires Prior Catchment Knowledge

Spatial differences in tracer expression are likely due to catchment characteristics impacting hydrologic routing, subsurface storage and mixing, and solute generation and modulation, as seen in catchments around the world (Beven et al. 1988; Botter et al. 2020; Jutebring Sterte et al. 2021; Musolff et al. 2015). Consistent with this framework, no solute met the tracer criteria in all three study catchments, indicating that there is no universal indicator of thaw depth. Instead, tracers likely need to be selected and calibrated on a catchment-to-catchment basis, and local geology and soil/land cover properties may help predict effective thaw tracers a priori. Whilst previous studies suspected certain tracers might work universally across the North Slope due to similarities in geology (Keller et al. 2010), our results show that tracer applicability varies across even directly adjacent catchments, highlighting the need for site-specific characterisation and validation.

Variability in tracer efficacy across the three study catchments can be explained by differences in lithology, soil properties and lake presence, each of which alters solute sources, flowpaths and residence times. Lithologic differences are particularly important for weathering-derived solutes. Na and S only met the tracer criteria in the *Alpine* catchment, likely reflecting enhanced weathering of shale and sandstone bedrock containing pyrite, a common sulphide mineral in the Brooks Range (Moore et al. 1986; Slack et al. 2021). Thickness of the organic soil horizon and thaw depth further regulate tracer expression by controlling the timing and extent of interaction between water and mineral soils. The *Alpine* catchment is characterised by thin organic soils and fractured bedrock that promote deeper thaw and greater thermal conductivity (Gruber and Haeberli 2007), conditions favourable for mobilising solutes such as Na and S from deeper mineral sources. In contrast, thicker organic horizons in the *Tundra* and *Lake-Influenced Tundra* catchments (Walker and Walker 1996) likely reduce contact with mineral soils, contributing to the low Na and S concentrations observed

10991085, 2026, 4, Downloaded from https://onlinelibrary.wiley.com/doi/10.1002/hyp.70512 by Jonathan O'Donnell , Wiley Online Library on [17/09/2026]. See the Terms and Conditions (https://onlinelibrary.wiley.com/terms-and-conditions) on Wiley Online Library for rules of use; OA articles are governed by the applicable Creative Commons License

throughout the thaw season (Figure 5). Whilst vegetation may also play a role in the cycling of some solutes, especially those that are limited in Arctic soils such as K (Chapin et al. 1975; Marion et al. 1989), vegetation differences likely do not strongly impact fluxes of these elements compared to the impacts of other catchment characteristics such as organic soil thickness. The differences in the *Lake-Influenced Tundra* catchment tracers versus the *Tundra* catchment tracers may be due to the presence of lakes, which modify solute behaviour by increasing water residence time, allowing for more solute reactions, degradation and sedimentation. Si specifically is often taken up by diatoms and undergoes sedimentation in lakes (Cornwell and Banahan 1992; Zahajská et al. 2021), likely reducing its ability to act as a tracer in the *Lake-Influenced* catchment which had over 10 times greater percent lake coverage than the other two catchments (Table 1). In contrast, Si concentrations in the *Alpine* catchment showed little seasonal variability (Figure 5), consistent with limited lake influence and rapid hydrologic routing associated with steep topography (Clow and Sueker 2000; McGuire et al. 2005). These examples of differences in effective tracers and factors that can regulate tracers beyond discharge and seasonality illustrate that thaw tracer selection must occur in the context of the catchment properties. Future thaw monitoring via this method might include a training period in each new region where a suite of potential tracers is evaluated, followed by a selection and calibration phase. Understanding catchment characteristics enables informed tracer selection and better transferability of this 'streams as sensors of thaw' approach to other permafrost regions.

4.3 | Future Directions

Whilst our stream tracer approach builds upon previous efforts, further refinements are needed to improve the tracing of thaw depth using these methods. One of the major questions with this approach is the spatial scale at which we can still detect ground thaw signals. Instream and near-stream processes can increasingly control stream chemistry as catchment size increases, overwriting soil chemical signals (Creed et al. 2015; Quinton and Pomeroy 2006; Wollheim et al. 2006). There are emerging methods to help determine the appropriate spatial scale for setting up *C*–*Q* monitoring to trace thaw depth at a particular site. For example, synoptic surveys at different nested scales (i.e., sampling a range of subcatchments making up a large catchment) can help determine where the variance collapses for a solute tracer, which indicates the spatial scale where different source or sink processes alter the stream chemistry (Abbott et al. 2018; Shogren et al. 2022; Weidner et al. 2025). This synoptic sampling approach might also help identify specific source locations (point-source) or more ubiquitous sourcing (diffuse source) of thaw tracer signals that are observed at larger scales like the catchment outlets of our study.

In general, the use of stream chemistry to detect thaw is possible because it is well-documented that solutes change in concentration with depth in the soil in the study region. Whilst we did not measure soil chemistry directly in this study, we leveraged previous soil chemistry data in this region (Barker et al. 2014; Keller et al. 2007; Lehn et al. 2017). Still, there is some uncertainty about how the soil chemistry data transfers between the three study catchments as there is not complete documentation of soil across these remote regions, which may be a factor in some of the variability and uncertainty we found in identifying effective tracers of thaw. Therefore, when considering the 'streams as sensors' approach in new permafrost regions, it is imperative to collect soil chemistry data to support the stream tracer work and aid in the selection of potentially effective tracers. Soil chemistry data can be collected via soil cores distributed throughout the catchment along with an integrated assessment of topography, surface geology and vegetation to help interpolate soil distribution. Additionally, whilst we obtained some direct thaw depth measurements to corroborate our tracer work, we do not know for certain if these measurements represented thaw depths and timing across the entire catchments, especially as soil and substrate properties may vary and thereby impact thaw and flowpath depths. In the future, pairing tracer work with techniques that can measure thaw more frequently and at broader spatial scales will enhance our approach, such as using synthetic aperture radar to measure ground thaw (Crevier et al. 2025; Sadeghi Chorsi et al. 2024) or ground-based monitoring networks like the CALM Network.

As with many simple models, GAMs modelling requires high quality data. Because the models are based on discharge and concentration data alone, they are impacted by errors in these data. In our case, the *Alpine* catchment had inferior rating curves compared to the other two catchments, which may lead to less certainty in the model results for the *Alpine* catchment. Better discharge measurements and more concentration data collected at a higher temporal resolution (e.g., sub-weekly) could improve model performance. The interpretation of the GAMs analysis is centred on the 'shallow and deep hypothesis' (Zhi and Li 2020), which represents a simplified framework of subsurface flowpaths. Here, we assumed *C*–*Q* relationships reflected this framework; however, it may be more complex at these sites. Future work could combine this study with coupled hydrogeochemical modelling to validate whether the processes align with this simple shallow and deep framework. Finally, despite significant *C*–*Q* slopes and sDOY terms in our results, it is possible there are other seasonal processes besides thaw driving seasonality, such as uptake in seasonal hyporheic zones (Brosten et al. 2006; Greenwald et al. 2008; Zarnetske et al. 2008). Analysing not only solute concentrations, but also other tracers such as isotopes or elemental ratios may provide more refined insights into how solute chemistry changes with flowpath depth, and therefore the efficacy of different solutes as tracers.

Overall, pursuing improvements of thaw depth tracing via this 'streams as sensors' technique and other methods is necessary for the Arctic research community to develop distributed, data-driven and process-based estimates of ground thaw dynamics. Our approach shows promise as a complementary approach to more spatially coarse (e.g., remote sensing) or fine-scale (e.g., frost probing) measurements of thaw depth.

5 | Conclusions

Ground thaw dynamics regulate many landscape and ecosystem processes across the Arctic; however, monitoring and modelling these dynamics is difficult in permafrost landscapes.

10991085, 2026, 4, Downloaded from https://onlinelibrary.wiley.com/doi/10.1002/hyp.70512 by Jonathan O'Donnell , Wiley Online Library on [17/09/2026]. See the Terms and Conditions (https://onlinelibrary.wiley.com/terms-and-conditions) on Wiley Online Library for rules of use; OA articles are governed by the applicable Creative Commons License

In this study, we showed that linking soil chemistry with seasonal trends in stream chemistry is a potentially useful tool to trace seasonal thaw at previously undocumented scales of mid-size catchments. However, we also observed that the efficacy of specific solutes as tracers is seemingly dependent on catchment characteristics and that there is no universally effective tracer of ground thaw. Mg, Na, S and Sr met effective tracer criteria in one catchment, whilst Ca met the criteria in both tundra catchments. Encouragingly, the *Alpine* catchment had three solutes that met tracer criteria and also happened to be the catchment where it was most difficult to record thaw depth through depth-to-resistance probing due to the rocky subsurface. Therefore, the use of thaw tracers may be a promising way forward in settings where thaw probing is difficult, as is often the case in steep alpine landscapes.

Tracing thaw depth with stream chemistry in permafrost catchments shows potential and necessitates more research and refinement. This study serves as a template for future studies aiming to develop catchment-scale thaw monitoring strategies by establishing a more robust framework and method for thaw tracers that accounts for previously confounding factors, such as variability in hydrologic conditions. Our results suggest that there is variation in the most effective thaw depth tracers between catchments with different properties, and therefore a suite of solutes must be tested in future study catchments to identify potential tracers. Other tracers of thaw depth that we did not analyse might also provide useful information, such as isotopes or additional trace elements. Future studies should also focus on the impacts of different catchment characteristics on stream chemistry in Arctic permafrost catchments, especially on elements that are typically more conservative tracers of thaw depth. Measuring and modelling thaw depth dynamics will become increasingly important as climate change impacts the Arctic and other permafrost regions. The stream tracer methods used in this study can be refined and used to detect not only seasonal-scale active layer thaw, but also longer scale permafrost thaw by monitoring long-term (multi-year) stream chemistry. Permafrost thaw has the potential to alter hydrologic connectivity, mobilise previously stored solute pools, and reshape biogeochemical cycling and water quality across Arctic landscapes and downstream aquatic systems. Therefore, we need to pursue additional tools to be able to predict thaw depth at short- and long-term scales, including using streams as sensors to link small-scale point-based ground measurements to emerging large-scale remote sensing measurements.

Acknowledgements

Support for this research was provided by Toolik Field Station, the Arctic LTER (NSF-DEB-2220863) and the Toolik Field Station Environmental Data Center and GIS staff. The authors would like to acknowledge A. Eichert, J. VerSteeg, C. Jones, J. Nipko, V. Prieto-Hurtado and G. Shoell for their fieldwork assistance. This work was funded by NSF-OPP-1916567 (J.P.Z. and A.J.S.), NSF-OPP-1916576 (W.B.B.), NSF-OPP-1916565 (B.W.A.) and NSF-EAR-1846855 (J.P.Z.). J.A.O. was supported by the National Park Service's Inventory & Monitoring Division and Water Resources Division. The study area is located on the ancestral hunting grounds and routes of the Nunamiut, Gwich'in, Koyukuk and Iñupiaq peoples.

Funding

This work was supported by the National Science Foundation (Grant Nos. NSF-OPP-1916567, NSF-OPP-1916576, NSF-OPP-1916565, NSF-EAR-1846855, NSF-DEB-2220863) and National Park Service.

Data Availability Statement

The stream chemistry and discharge point data used in the GAMs analysis are publicly available through CUAHSI HydroShare at: https://doi.org/10.4211/hs.5ad0062a801f406a882b7eebf71be1d9 (Grose et al. 2026).

References

Abbott, B. W., G. Gruau, J. P. Zarnetske, et al. 2018. "Unexpected Spatial Stability of Water Chemistry in Headwater Stream Networks." *Ecology Letters* 21, no. 2: 296–308. https://doi.org/10.1111/ele.12897.

Ackerman, D. E., and J. C. Finlay. 2019. "Road Dust Biases NDVI and Alters Edaphic Properties in Alaskan Arctic Tundra." *Scientific Reports* 9, no. 1: 214. https://doi.org/10.1038/s41598-018-36804-3.

Anisimov, O. A., N. I. Shiklomanov, and F. E. Nelson. 1997. "Global Warming and Active-Layer Thickness: Results From Transient General Circulation Models." *Global and Planetary Change* 15, no. 3–4: 61–77. https://doi.org/10.1016/S0921-8181(97)00009-X.

Arp, C. D., M. S. Whitman, R. Kemnitz, and S. L. Stuefer. 2020. "Evidence of Hydrological Intensification and Regime Change From Northern Alaskan Watershed Runoff." *Geophysical Research Letters* 47, no. 17: e2020GL089186. https://doi.org/10.1029/2020GL089186.

Barker, A. J., T. A. Douglas, A. D. Jacobson, et al. 2014. "Late Season Mobilization of Trace Metals in Two Small Alaskan Arctic Watersheds as a Proxy for Landscape Scale Permafrost Active Layer Dynamics." *Chemical Geology* 381: 180–193. https://doi.org/10.1016/j.chemgeo.2014.05.012.

Beusen, A. H. W., A. F. Bouwman, H. H. Dürr, A. L. M. Dekkers, and J. Hartmann. 2009. "Global Patterns of Dissolved Silica Export to the Coastal Zone: Results From a Spatially Explicit Global Model." *Global Biogeochemical Cycles* 23, no. 4: GB0A02. https://doi.org/10.1029/2008gb003281.

Beven, K. J., E. F. Wood, and M. Sivapalan. 1988. "On Hydrological Heterogeneity—Catchment Morphology and Catchment Response." *Journal of Hydrology* 100, no. 1–3: 353–375. https://doi.org/10.1016/0022-1694(88)90192-8.

Bintanja, R., and O. Andry. 2017. "Towards a Rain-Dominated Arctic." *Nature Climate Change* 7, no. 4: 263–267. https://doi.org/10.1038/nclimate3240.

Blackburn, M., J. L. J. Ledesma, T. Näsholm, H. Laudon, and R. A. Sponseller. 2017. "Evaluating Hillslope and Riparian Contributions to Dissolved Nitrogen (N) Export From a Boreal Forest Catchment." *Journal of Geophysical Research: Biogeosciences* 122, no. 2: 324–339. https://doi.org/10.1002/2016JG003535.

Boike, J., S. Chadburn, J. Martin, et al. 2022. "Standardized Monitoring of Permafrost Thaw: A User-Friendly, Multiparameter Protocol." *Arctic Science* 8, no. 1: 153–182. https://doi.org/10.1139/as-2021-0007.

Botter, M., L. Li, J. Hartmann, P. Burlando, and S. Fatichi. 2020. "Depth of Solute Generation is a Dominant Control on Concentration-Discharge Relations." *Water Resources Research* 56, no. 8: e2019WR026695. https://doi.org/10.1029/2019WR026695.

Bowden, W. B., M. J. Greenwald, M. N. Gooseff, et al. 2008. "Carbon, Nitrogen, and Phosphorus Interactions in the Hyporheic Zone of Arctic Stream That Drain Areas of Continuous Permafrost." In *Proceedings of the Ninth International Conference on Permafrost*, University of Alaska Fairbanks, June 29–July 3, 165–170.

10991085, 2026, 4, Downloaded from https://onlinelibrary.wiley.com/doi/10.1002/hyp.70512 by Jonathan O'Donnell , Wiley Online Library on [17/09/2026]. See the Terms and Conditions (https://onlinelibrary.wiley.com/terms-and-conditions) on Wiley Online Library for rules of use; OA articles are governed by the applicable Creative Commons License

Bring, A., I. Fedorova, Y. Dibike, et al. 2016. "Arctic Terrestrial Hydrology: A Synthesis of Processes, Regional Effects, and Research Challenges." *Journal of Geophysical Research: Biogeosciences* 121, no. 3: 621–649. https://doi.org/10.1002/2015JG003131.

Brosten, T. R., J. H. Bradford, J. P. McNamara, J. P. Zarnetske, M. N. Gooseff, and W. B. Bowden. 2006. "Profiles of Temporal Thaw Depths Beneath Two Arctic Stream Types Using Ground-Penetrating Radar." *Permafrost and Periglacial Processes* 17, no. 4: 341–355. https://doi.org/10.1002/ppp.566.

Brown, J., K. M. Hinkel, and F. E. Nelson. 2000. "The Circumpolar Active Layer Monitoring (Calm) Program: Research Designs and Initial Results." *Polar Geography* 24, no. 3: 166–258. https://doi.org/10.1080/10889370009377698.

Carey, J. C., J. Gewirtzman, S. E. Johnston, et al. 2020. "Arctic River Dissolved and Biogenic Silicon Exports—Current Conditions and Future Changes With Warming." *Global Biogeochemical Cycles* 34, no. 3: e2019GB006308. https://doi.org/10.1029/2019gb006308.

Carey, S., J. Boucher, and C. Duarte. 2013. "Inferring Groundwater Contributions and Pathways to Streamflow During Snowmelt Over Multiple Years in a Discontinuous Permafrost Subarctic Environment (Yukon, Canada)." *Hydrogeology Journal* 21, no. 1: 67–77. https://doi.org/10.1007/s10040-012-0920-9.

Carey, S., and M. Woo. 1999. "Hydrology of Two Slopes in Subarctic Yukon, Canada." *Hydrological Processes* 13, no. 16: 2549–2562. https://doi.org/10.1002/(SICI)1099-1085(199911)13:16<2549::AID-HYP938>3.0.CO;2-H.

Chapin, F. S., K. Van Cleve, and L. L. Tieszen. 1975. "Seasonal Nutrient Dynamics of Tundra Vegetation at Barrow, Alaska." *Arctic and Alpine Research* 7, no. 3: 209–226. https://doi.org/10.1080/00040851.1975.12003828.

Chen, J., Y. Wu, M. O'Connor, et al. 2020. "Active Layer Freeze-Thaw and Water Storage Dynamics in Permafrost Environments Inferred From InSAR." *Remote Sensing of Environment* 248: 112007. https://doi.org/10.1016/j.rse.2020.112007.

Chiasson-Poirier, G., J. Franssen, M. Lafrenière, D. Fortier, and S. Lamoureux. 2020. "Seasonal Evolution of Active Layer Thaw Depth and Hillslope-Stream Connectivity in a Permafrost Watershed." *Water Resources Research* 56, no. 1: e2019WR025828. https://doi.org/10.1029/2019WR025828.

Clayton, L. K., K. Schaefer, M. J. Battaglia, et al. 2021. "Active Layer Thickness as a Function of Soil Water Content." *Environmental Research Letters* 16, no. 5: 055028. https://doi.org/10.1088/1748-9326/abfa4c.

Clow, D. W., and J. K. Sueker. 2000. "Relations Between Basin Characteristics and Stream Water Chemistry in Alpine/Subalpine Basins in Rocky Mountain National Park, Colorado." *Water Resources Research* 36, no. 1: 49–61. https://doi.org/10.1029/1999WR900294.

Colombo, N., F. Salerno, S. Gruber, et al. 2018. "Review: Impacts of Permafrost Degradation on Inorganic Chemistry of Surface Fresh Water." *Global and Planetary Change* 162: 69–83. https://doi.org/10.1016/j.gloplacha.2017.11.017.

Condon, L. E., K. H. Markovich, C. A. Kelleher, J. J. McDonnell, G. Ferguson, and J. C. McIntosh. 2020. "Where is the Bottom of a Watershed?" *Water Resources Research* 56, no. 3: e2019WR026010. https://doi.org/10.1029/2019WR026010.

Cooper, M. G., T. Zhou, K. E. Bennett, et al. 2023. "Detecting Permafrost Active Layer Thickness Change From Nonlinear Baseflow Recession." *Water Resources Research* 59, no. 1: e2022WR033154. https://doi.org/10.1029/2022WR033154.

Cornwell, J. C. 1992. "Cation Export From Alaskan Arctic Watersheds." *Hydrobiologia* 240: 15–22.

Cornwell, J. C., and S. Banahan. 1992. "A Silicon Budget for an Alaskan Arctic Lake." *Hydrobiologia* 240, no. 1: 37–44. https://doi.org/10.1007/BF00013450.

Creed, I. F., D. M. McKnight, B. A. Pellerin, et al. 2015. "The River as a Chemostat: Fresh Perspectives on Dissolved Organic Matter Flowing Down the River Continuum." *Canadian Journal of Fisheries and Aquatic Sciences* 72, no. 8: 1272–1285. https://doi.org/10.1139/cjfas-2014-0400.

Crevier, C., A. Langlois, C. Derksen, and A. Roy. 2025. "A Multisensor C-Band Synthetic Aperture Radar (SAR) Approach to Retrieve Freeze/Thaw Cycles: A Case Study for a Low Arctic Environment." Preprint, EGUsphere. https://doi.org/10.5194/egusphere-2024-3580.

Davis, S. N. 1964. "Silica in Streams and Ground Water." *American Journal of Science* 262: 870–891.

Dingman, S. L. 1973. "Effects of Permafrost on Stream Flow Characteristics in the Discontinuous Permafrost Zone of Central Alaska." In *Proceedings of Permafrost: North American Contribution to the Second International Conference*, 447–453. NAS.

Dunne, T., and R. D. Black. 1970. "Partial Area Contributions to Storm Runoff in a Small New England Watershed." *Water Resources Research* 6, no. 5: 1296–1311. https://doi.org/10.1029/WR006i005p01296.

Emerson, D., J. J. Scott, J. Benes, and W. B. Bowden. 2015. "Microbial Iron Oxidation in the Arctic Tundra and Its Implications for Biogeochemical Cycling." *Applied and Environmental Microbiology* 81, no. 23: 8066–8075. https://doi.org/10.1128/AEM.02832-15.

Everett, K. R., G. M. Marion, and D. L. Kane. 1989. "Seasonal Geochemistry of an Arctic Tundra Drainage Basin." *Ecography* 12, no. 3: 279–289. https://doi.org/10.1111/j.1600-0587.1989.tb00847.x.

Frey, K. E., and J. W. McClelland. 2009. "Impacts of Permafrost Degradation on Arctic River Biogeochemistry." *Hydrological Processes* 23, no. 1: 169–182. https://doi.org/10.1002/hyp.7196.

Frey, K. E., J. W. McClelland, R. M. Holmes, and L. C. Smith. 2007. "Impacts of Climate Warming and Permafrost Thaw on the Riverine Transport of Nitrogen and Phosphorus to the Kara Sea." *Journal of Geophysical Research: Biogeosciences* 112, no. G4: 2006JG000369. https://doi.org/10.1029/2006JG000369.

Gödde, A., B. Moe, and Ø. Mikkelsen. 2024. "Seasonal Dynamics of Chemistry in an Arctic Glacier-Fed River." *Science of the Total Environment* 954: 176645. https://doi.org/10.1016/j.scitotenv.2024.176645.

Godsey, S. E., J. W. Kirchner, and D. W. Clow. 2009. "Concentration–Discharge Relationships Reflect Chemostatic Characteristics of US Catchments." *Hydrological Processes* 23, no. 13: 1844–1864. https://doi.org/10.1002/hyp.7315.

Greenwald, M. J., W. B. Bowden, M. N. Gooseff, et al. 2008. "Hyporheic Exchange and Water Chemistry of Two Arctic Tundra Streams of Contrasting Geomorphology." *Journal of Geophysical Research: Biogeosciences* 113, no. G2: 2007JG000549. https://doi.org/10.1029/2007JG000549.

Grewal, A., E. M. Nicholls, and S. K. Carey. 2025. "The Role of Catchment Characteristics, Discharge, and Active- Layer Thaw in Seasonal Stream Chemistry Across 10 Permafrost Catchments." *Hydrology and Earth System Sciences* 29, no. 11: 2467–2483. https://doi.org/10.5194/hess-29-2467-2025.

Grewal, A. S., C. J. Harman, and S. K. Carey. 2025. "Water Storage and Release in Permafrost Catchments: Insights From Hydrometrics, End-Member Mixing, and Water Age Characterization." *Water Resources Research* 61: e2024WR038957. https://doi.org/10.1029/2024WR038957.

Grose, A., A. Rec, A. Shogren, et al. 2026. "Stream Geochemistry Data for Three Arctic Headwater Streams, North Slope, Alaska, 2021–2023." [Dataset]. *HydroShare*. http://www.hydroshare.org/resource/5ad0062a801f406a882b7eebf71be1d9.

Gruber, S., and W. Haeberli. 2007. "Permafrost in Steep Bedrock Slopes and Its Temperature-Related Destabilization Following Climate Change." *Journal of Geophysical Research: Earth Surface* 112, no. F2: 2006JF000547. https://doi.org/10.1029/2006JF000547.

10991085, 2026, 4, Downloaded from https://onlinelibrary.wiley.com/doi/10.1002/hyp.70512 by Jonathan O'Donnell , Wiley Online Library on [17/09/2026]. See the Terms and Conditions (https://onlinelibrary.wiley.com/terms-and-conditions) on Wiley Online Library for rules of use; OA articles are governed by the applicable Creative Commons License

Hamilton, T. D. 2003. "Glacial Geology of the Toolik Lake and Upper Kuparuk River Regions." In *Geobotanical Atlas of the Kuparuk River Region*, 1–25. Institute of Arctic Biology, University of Alaska.

Harms, T. K., and J. B. Jones Jr. 2012. "Thaw Depth Determines Reaction and Transport of Inorganic Nitrogen in Valley Bottom Permafrost Soils." *Global Change Biology* 18, no. 9: 2958–2968. https://doi.org/10.1111/j.1365-2486.2012.02731.x.

Herndon, E., A. AlBashaireh, D. Singer, T. Roy Chowdhury, B. Gu, and D. Graham. 2017. "Influence of Iron Redox Cycling on Organo-Mineral Associations in Arctic Tundra Soil." *Geochimica et Cosmochimica Acta* 207: 210–231. https://doi.org/10.1016/j.gca.2017.02.034.

Hewlett, J. D., and A. R. Hibbert. 1967. "Factors Affecting the Response of Small Watersheds to Precipitation in Humid Areas." In *Forest Hydrology*, 275–290. Pergamon Press. https://doi.org/10.1177/030913330933833 8118.

Hinzman, A. M., Y. Sjöberg, S. W. Lyon, S. W. Ploum, and Y. Van Der Velde. 2020. "Increasing Non-Linearity of the Storage-Discharge Relationship in Sub-Arctic Catchments." *Hydrological Processes* 34, no. 19: 3894–3909. https://doi.org/10.1002/hyp.13860.

Hinzman, L. D., D. J. Goering, and D. L. Kane. 1998. "A Distributed Thermal Model for Calculating Soil Temperature Profiles and Depth of Thaw in Permafrost Regions." *Journal of Geophysical Research: Atmospheres* 103, no. D22: 28975–28991. https://doi.org/10.1029/98JD01731.

Hinzman, L. D., D. L. Kane, R. E. Gieck, and K. R. Everett. 1991. "Hydrologic and Thermal Properties of the Active Layer in the Alaskan Arctic." *Cold Regions Science and Technology* 19, no. 2: 95–110. https://doi.org/10.1016/0165-232X(91)90001-W.

Huryn, A. D., and J. E. Hobbie. 2012. *Land of Extremes: A Natural History of the Arctic North Slope of Alaska*. University of Alaska Press.

Johnson, L., C. Richards, G. Host, and J. Arthur. 1997. "Landscape Influences on Water Chemistry in Midwestern Stream Ecosystems." *Freshwater Biology* 37, no. 1: 193–208. https://doi.org/10.1046/j.1365-2427.1997.d01-539.x.

Jorgenson, M. T., J. E. Roth, P. F. Miller, et al. 2009. *An Ecological Land Survey and Landcover Map of the Arctic Network* (Natural Resource Technical Report NPS/ARCN/NRTR—2009/270). National Park Service, Natural Resource Stewardship and Science. https://irma.nps.gov/DataStore/Reference/Profile/663934.

Jutebring Sterte, E., F. Lidman, E. Lindborg, Y. Sjöberg, and H. Laudon. 2021. "How Catchment Characteristics Influence Hydrological Pathways and Travel Times in a Boreal Landscape." *Hydrology and Earth System Sciences* 25, no. 4: 2133–2158. https://doi.org/10.5194/hess-25-2133-2021.

Kane, D. L., L. D. Hinzman, and J. P. Zarling. 1991. "Thermal Response of the Active Layer to Climatic Warming in a Permafrost Environment." *Cold Regions Science and Technology* 19, no. 2: 111–122. https://doi.org/10.1016/0165-232X(91)90002-X.

Kane, D. L., K. Yoshikawa, and J. P. McNamara. 2013. "Regional Groundwater Flow in an Area Mapped as Continuous Permafrost, NE Alaska (USA)." *Hydrogeology Journal* 21, no. 1: 41–52. https://doi.org/10.1007/s10040-012-0937-0.

Keller, K., J. D. Blum, and G. W. Kling. 2007. "Geochemistry of Soils and Streams on Surfaces of Varying Ages in Arctic Alaska." *Arctic, Antarctic, and Alpine Research* 39, no. 1: 84–98. https://doi.org/10.1657/1523-0430(2007)39[84:GOSASO]2.0.CO;2.

Keller, K., J. D. Blum, and G. W. Kling. 2010. "Stream Geochemistry as an Indicator of Increasing Permafrost Thaw Depth in an Arctic Watershed." *Chemical Geology* 273, no. 1–2: 76–81. https://doi.org/10.1016/j.chemgeo.2010.02.013.

Khosh, M. S., J. W. McClelland, A. D. Jacobson, T. A. Douglas, A. J. Barker, and G. O. Lehn. 2017. "Seasonality of Dissolved Nitrogen From Spring Melt to Fall Freezeup in Alaskan Arctic Tundra and Mountain Streams." *Journal of Geophysical Research: Biogeosciences* 122, no. 7: 1718–1737. https://doi.org/10.1002/2016JG003377.

King, T., B. Neilson, L. Overbeck, and D. Kane. 2020. "A Distributed Analysis of Lateral Inflows in an Alaskan Arctic Watershed Underlain by Continuous Permafrost." *Hydrological Processes* 34, no. 3: 633–648. https://doi.org/10.1002/hyp.13611.

Kling, G. W. 2025. *Imnavait Watershed Thaw Depth Survey Summary for 2003 to 2024, Arctic LTER, Toolik Research Station, Alaska* (Version 13) [Dataset]. Environmental Data Initiative.

Knapp, J. L. A., L. Li, and A. Musolff. 2022. "Hydrologic Connectivity and Source Heterogeneity Control Concentration–Discharge Relationships." *Hydrological Processes* 36, no. 9: e14683. https://doi.org/10.1002/hyp.14683.

Koch, J., C. Connolly, C. Baughman, M. Repasch, H. Best, and A. Hunt. 2024. "The Dominance and Growth of Shallow Groundwater Resources in Continuous Permafrost Environments." *Proceedings of the National Academy of Sciences of the United States of America* 121, no. 23: e2317873121. https://doi.org/10.1073/pnas.2317873121.

Koch, J. C., Y. Sjöberg, J. A. O'Donnell, M. P. Carey, P. F. Sullivan, and A. Terskaia. 2022. "Sensitivity of Headwater Streamflow to Thawing Permafrost and Vegetation Change in a Warming Arctic." *Environmental Research Letters* 17, no. 4: 044074. https://doi.org/10.1088/1748-9326/ac5f2d.

Lafrenière, M. J., and S. F. Lamoureux. 2019. "Effects of Changing Permafrost Conditions on Hydrological Processes and Fluvial Fluxes." *Earth-Science Reviews* 191: 212–223. https://doi.org/10.1016/j.earscirev.2019.02.018.

Ledesma, J. L. J., D. N. Kothawala, P. Bastviken, S. Maehder, T. Grabs, and M. N. Futter. 2018. "Stream Dissolved Organic Matter Composition Reflects the Riparian Zone, Not Upslope Soils in Boreal Forest Headwaters." *Water Resources Research* 54, no. 6: 3896–3912. https://doi.org/10.1029/2017WR021793.

Lehn, G. O., A. D. Jacobson, T. A. Douglas, J. W. McClelland, A. J. Barker, and M. S. Khosh. 2017. "Constraining Seasonal Active Layer Dynamics and Chemical Weathering Reactions Occurring in North Slope Alaskan Watersheds With Major Ion and Isotope ($\delta^{34}S_{SO4}$, $\delta^{13}C$-$_{DIC}$, $^{87}Sr/^{86}Sr$, $\delta^{44/40}Ca$, and $\delta^{44/42}Ca$) Measurements." *Geochimica et Cosmochimica Acta* 217: 399–420. https://doi.org/10.1016/j.gca.2017.07.042.

Lewkowicz, A. G., and H. French. 1982. "The Hydrology of Small Runoff Plots in an Area of Continuous Permafrost, Banks Island, N.W.T." In *4th Canadian Permafrost Conference*, 151–162.

Li, L., C. Bao, P. L. Sullivan, S. Brantley, Y. Shi, and C. Duffy. 2017. "Understanding Watershed Hydrogeochemistry: 2. Synchronized Hydrological and Geochemical Processes Drive Stream Chemostatic Behavior." *Water Resources Research* 53, no. 3: 2346–2367. https://doi.org/10.1002/2016WR018935.

Luo, D., Q. Wu, H. Jin, S. S. Marchenko, L. Lü, and S. Gao. 2016. "Recent Changes in the Active Layer Thickness Across the Northern Hemisphere." *Environmental Earth Sciences* 75, no. 7: 555. https://doi.org/10.1007/s12665-015-5229-2.

MacLean, R., M. W. Oswood, J. G. Irons, and W. H. McDowell. 1999. "The Effect of Permafrost on Stream Biogeochemistry: A Case Study of Two Streams in the Alaskan (U.S.A.) Taiga." *Biogeochemistry* 47, no. 3: 239–267. https://doi.org/10.1007/BF00992909.

Maher, K., and C. P. Chamberlain. 2014. "Hydrologic Regulation of Chemical Weathering and the Geologic Carbon Cycle." *Science* 343, no. 6178: 1502–1504. https://doi.org/10.1126/science.1250770.

Marion, G. M., S. J. Hastings, S. F. Oberbauer, and W. C. Oechel. 1989. "Soil-Plant Element Relationships in a Tundra Ecosystem." *Holarctic Ecology* 12, no. 3: 296–303.

10991085, 2026, 4, Downloaded from https://onlinelibrary.wiley.com/doi/10.1002/hyp.70512 by Jonathan O'Donnell , Wiley Online Library on [17/09/2026]. See the Terms and Conditions (https://onlinelibrary.wiley.com/terms-and-conditions) on Wiley Online Library for rules of use; OA articles are governed by the applicable Creative Commons License

McGuire, K. J., J. J. McDonnell, M. Weiler, et al. 2005. "The Role of Topography on Catchment-Scale Water Residence Time." *Water Resources Research* 41, no. 5: 2004WR003657. https://doi.org/10.1029/2004WR003657.

McKnight, D. M., B. A. Kimball, and K. E. Bencala. 1988. "Iron Photoreduction and Oxidation in an Acidic Mountain Stream." *Science* 240, no. 4852: 637–640. https://doi.org/10.1126/science.240.4852.637.

McNamara, J., D. Kane, and L. Hinzman. 1997. "Hydrograph Separations in an Arctic Watershed Using Mixing Model and Graphical Techniques." *Water Resources Research* 33, no. 7: 1707–1719. https://doi.org/10.1029/97WR01033.

McNamara, J., D. Kane, and L. Hinzman. 1998. "An Analysis of Streamflow Hydrology in the Kuparuk River Basin, Arctic Alaska: A Nested Watershed Approach." *Journal of Hydrology* 206, no. 1–2: 39–57. https://doi.org/10.1016/S0022-1694(98)00083-3.

Michalek, A. T., G. Villarini, A. F. Prein, J. M. Done, D. R. Johnson, and C. Wang. 2025. "Precipitation- and Temperature-Driven Future Changes to Flooding in Alaska." *Geophysical Research Letters* 52, no. 3: e2024GL112004. https://doi.org/10.1029/2024GL112004.

Michaud, A. B., R. O. Massé, and D. Emerson. 2023. "Microbial Iron Cycling is Prevalent in Water-Logged Alaskan Arctic Tundra Habitats, but Sensitive to Disturbance." *FEMS Microbiology Ecology* 99, no. 3: fiad013. https://doi.org/10.1093/femsec/fiad013.

Moatar, F., B. W. Abbott, C. Minaudo, F. Curie, and G. Pinay. 2017. "Elemental Properties, Hydrology, and Biology Interact to Shape Concentration-Discharge Curves for Carbon, Nutrients, Sediment, and Major Ions." *Water Resources Research* 53, no. 2: 1270–1287. https://doi.org/10.1002/2016WR019635.

Moore, D. W., L. E. Young, J. S. Modene, and J. T. Plahuta. 1986. "Geologic Setting and Genesis of the Red Dog Zinc-Lead-Silver Deposit, Western Brooks Range, Alaska." *Economic Geology* 81, no. 7: 1696–1727. https://doi.org/10.2113/gsecongeo.81.7.1696.

Musolff, A., C. Schmidt, B. Selle, and J. H. Fleckenstein. 2015. "Catchment Controls on Solute Export." *Advances in Water Resources* 86: 133–146. https://doi.org/10.1016/j.advwatres.2015.09.026.

Myrstener, M., G. Rocher-Ros, R. M. Burrows, A. Bergström, R. Giesler, and R. A. Sponseller. 2018. "Persistent Nitrogen Limitation of Stream Biofilm Communities Along Climate Gradients in the Arctic." *Global Change Biology* 24, no. 8: 3680–3691. https://doi.org/10.1111/gcb.14117.

Nelson, F. E., N. I. Shiklomanov, G. R. Mueller, K. M. Hinkel, D. A. Walker, and J. G. Bockheim. 1997. "Estimating Active-Layer Thickness Over a Large Region: Kuparuk River Basin, Alaska, U.S.A." *Arctic and Alpine Research* 29, no. 4: 367. https://doi.org/10.2307/1551985.

Nyland, K. E., N. I. Shiklomanov, D. A. Streletskiy, F. E. Nelson, A. E. Klene, and A. L. Kholodov. 2021. "Long-Term Circumpolar Active Layer Monitoring (CALM) Program Observations in Northern Alaskan Tundra." *Polar Geography* 44, no. 3: 167–185. https://doi.org/10.1080/1088937X.2021.1988000.

Obu, J. 2021. "How Much of the Earth's Surface is Underlain by Permafrost?" *Journal of Geophysical Research: Earth Surface* 126, no. 5: e2021JF006123. https://doi.org/10.1029/2021JF006123.

O'Connor, M. T., M. B. Cardenas, B. T. Neilson, K. D. Nicholaides, and G. W. Kling. 2019. "Active Layer Groundwater Flow: The Interrelated Effects of Stratigraphy, Thaw, and Topography." *Water Resources Research* 55, no. 8: 6555–6576. https://doi.org/10.1029/2018WR024636.

O'Donnell, J. A., G. R. Aiken, M. A. Walvoord, et al. 2014. "Using Dissolved Organic Matter Age and Composition to Detect Permafrost Thaw in Boreal Watersheds of Interior Alaska." *Journal of Geophysical Research: Biogeosciences* 119, no. 11: 2155–2170. https://doi.org/10.1002/2014JG002695.

O'Donnell, J. A., M. P. Carey, J. C. Koch, et al. 2024. "Metal Mobilization From Thawing Permafrost to Aquatic Ecosystems is Driving Rusting of Arctic Streams." *Communications Earth & Environment* 5, no. 1: 1–10. https://doi.org/10.1038/s43247-024-01446-z.

Osterkamp, T. E., and M. W. Payne. 1981. "Estimates of Permafrost Thickness From Well Logs in Northern Alaska." *Cold Regions Science and Technology* 5, no. 1: 13–27. https://doi.org/10.1016/0165-232X(81)90037-9.

Petrone, K. C., J. B. Jones, L. D. Hinzman, and R. D. Boone. 2006. "Seasonal Export of Carbon, Nitrogen, and Major Solutes From Alaskan Catchments With Discontinuous Permafrost." *Journal of Geophysical Research: Biogeosciences* 111, no. G2: 2005JG000055. https://doi.org/10.1029/2005JG000055.

Quinton, W., and P. Marsh. 1999. "A Conceptual Framework for Runoff Generation in a Permafrost Environment." *Hydrological Processes* 13, no. 16: 2563–2581. https://doi.org/10.1002/(SICI)1099-1085(199911)13:16<2563::AID-HYP942>3.0.CO;2-D.

Quinton, W., and J. Pomeroy. 2006. "Transformations of Runoff Chemistry in the Arctic Tundra, Northwest Territories, Canada." *Hydrological Processes* 20, no. 14: 2901–2919. https://doi.org/10.1002/hyp.6083.

Rantanen, M., A. Y. Karpechko, A. Lipponen, et al. 2022. "The Arctic Has Warmed Nearly Four Times Faster Than the Globe Since 1979." *Communications Earth & Environment* 3, no. 1: 1–10. https://doi.org/10.1038/s43247-022-00498-3.

Rawlins, M. A., and A. V. Karmalkar. 2024. "Regime Shifts in Arctic Terrestrial Hydrology Manifested From Impacts of Climate Warming." *Cryosphere* 18, no. 3: 1033–1052. https://doi.org/10.5194/tc-18-1033-2024.

Reimann, C., P. Filzmoser, R. G. Garrett, and R. Dutter. 2008. "Preparing the Data for Use in R and DAS+R." In *Statistical Data Analysis Explained: Applied Environmental Statistics With R*, 13–28. Wiley. https://doi.org/10.1002/9780470987605.

Reyes, F. R., and V. L. Lougheed. 2015. "Rapid Nutrient Release From Permafrost Thaw in Arctic Aquatic Ecosystems." *Arctic, Antarctic, and Alpine Research* 47, no. 1: 35–48. https://doi.org/10.1657/AAAR0013-099.

Romanowicz, K. J., and G. W. Kling. 2022. "Summer Thaw Duration is a Strong Predictor of the Soil Microbiome and Its Response to Permafrost Thaw in Arctic Tundra." *Environmental Microbiology* 24, no. 12: 6220–6237. https://doi.org/10.1111/1462-2920.16218.

Sadeghi Chorsi, T., F. J. Meyer, and T. H. Dixon. 2024. "Toward Long-Term Monitoring of Regional Permafrost Thaw With Satellite Interferometric Synthetic Aperture Radar." *Cryosphere* 18, no. 8: 3723–3740. https://doi.org/10.5194/tc-18-3723-2024.

Schuur, E. A. G., B. W. Abbott, R. Commane, et al. 2022. "Permafrost and Climate Change: Carbon Cycle Feedbacks From the Warming Arctic." *Annual Review of Environment and Resources* 47, no. 1: 343–371. https://doi.org/10.1146/annurev-environ-012220-011847.

Shaver, G. R., and F. S. Chapin. 1980. "Response to Fertilization by Various Plant Growth Forms in an Alaskan Tundra: Nutrient Accumulation and Growth." *Ecology* 61, no. 3: 662–675. https://doi.org/10.2307/1937432.

Shaver, G. R., F. Chapin III, and B. L. Gartner. 1986. "Factors Limiting Seasonal Growth and Peak Biomass Accumulation in *Eriophorum vaginatum* in Alaskan Tussock Tundra." *Journal of Ecology* 74, no. 1: 257–278. https://doi.org/10.2307/2260362.

Shiklomanov, N. I. 2025. *Seasonal Soil Active Layer Measurements From a Circumpolar Active Layer Monitoring (CALM) Grid, (U11a) Imnavait Creek 1 Kilometer Grid, Alaska, 1995-2024* [Dataset]. Arctic Data Center. https://doi.org/10.18739/A2XG9FD0J.

Shogren, A. J., J. P. Zarnetske, B. W. Abbott, et al. 2019. "Revealing Biogeochemical Signatures of Arctic Landscapes With River

10991085, 2026, 4, Downloaded from https://onlinelibrary.wiley.com/doi/10.1002/hyp.70512 by Jonathan O'Donnell , Wiley Online Library on [17/09/2026]. See the Terms and Conditions (https://onlinelibrary.wiley.com/terms-and-conditions) on Wiley Online Library for rules of use; OA articles are governed by the applicable Creative Commons License

Chemistry." *Scientific Reports* 9, no. 1: 12894. https://doi.org/10.1038/s41598-019-49296-6.

Shogren, A. J., J. P. Zarnetske, B. W. Abbott, et al. 2021. "Arctic Concentration–Discharge Relationships for Dissolved Organic Carbon and Nitrate Vary With Landscape and Season." *Limnology and Oceanography* 66, no. S1: S197–S215. https://doi.org/10.1002/lno.11682.

Shogren, A. J., J. P. Zarnetske, B. W. Abbott, et al. 2022. "Multi-Year, Spatially Extensive, Watershed-Scale Synoptic Stream Chemistry and Water Quality Conditions for Six Permafrost-Underlain Arctic Watersheds." *Earth System Science Data* 14, no. 1: 95–116. https://doi.org/10.5194/essd-14-95-2022.

Skierszkan, E. K., S. K. Carey, S. I. Jackson, M. Fellwock, C. Fraser, and M. B. J. Lindsay. 2024. "Seasonal Controls on Stream Metal(Loid) Signatures in Mountainous Discontinuous Permafrost." *Science of the Total Environment* 908: 167999. https://doi.org/10.1016/j.scitotenv.2023.167999.

Skierszkan, E. K., J. W. Dockrey, and M. B. J. Lindsay. 2024. "Metal Mobilization From Thawing Permafrost is an Emergent Risk to Water Resources." *ACS ES&T Water* 5: 20–32. https://doi.org/10.1021/acestwater.4c00789.

Slack, J. F., R. J. McAleer, W. C. Shanks, and J. A. Dumoulin. 2021. "Diagenetic Barite-Pyrite-Wurtzite Formation and Redox Signatures in Triassic Mudstone, Brooks Range, Northern Alaska." *Chemical Geology* 585: 120568. https://doi.org/10.1016/j.chemgeo.2021.120568.

Smith, A. A., D. Tetzlaff, and C. Soulsby. 2020. "Using Storage Selection Functions to Assess Mixing Patterns and Water Ages of Soil Water, Evaporation and Transpiration." *Advances in Water Resources* 141: 103586. https://doi.org/10.1016/j.advwatres.2020.103586.

Spence, C., X. Guan, R. Phillips, N. Hedstrom, R. Granger, and B. Reid. 2010. "Storage Dynamics and Streamflow in a Catchment With a Variable Contributing Area." *Hydrological Processes* 24, no. 16: 2209–2221. https://doi.org/10.1002/hyp.7492.

Stewart, B., J. B. Shanley, J. W. Kirchner, et al. 2022. "Streams as Mirrors: Reading Subsurface Water Chemistry From Stream Chemistry." *Water Resources Research* 58, no. 1: e2021WR029931. https://doi.org/10.1029/2021WR029931.

Striegl, R. G., G. R. Aiken, M. M. Dornblaser, P. A. Raymond, and K. P. Wickland. 2005. "A Decrease in Discharge-Normalized DOC Export by the Yukon River During Summer Through Autumn." *Geophysical Research Letters* 32, no. 21: 2005GL024413. https://doi.org/10.1029/2005GL024413.

Tank, S. E., J. W. McClelland, R. G. M. Spencer, et al. 2023. "Recent Trends in the Chemistry of Major Northern Rivers Signal Widespread Arctic Change." *Nature Geoscience* 16, no. 9: 789–796. https://doi.org/10.1038/s41561-023-01247-7.

Tank, S. E., J. E. Vonk, M. A. Walvoord, J. W. McClelland, I. Laurion, and B. W. Abbott. 2020. "Landscape Matters: Predicting the Biogeochemical Effects of Permafrost Thaw on Aquatic Networks With a State Factor Approach." *Permafrost and Periglacial Processes* 31, no. 3: 358–370. https://doi.org/10.1002/ppp.2057.

Toohey, R. C., N. M. Herman-Mercer, P. F. Schuster, E. A. Mutter, and J. C. Koch. 2016. "Multidecadal Increases in the Yukon River Basin of Chemical Fluxes as Indicators of Changing Flowpaths, Groundwater, and Permafrost." *Geophysical Research Letters* 43, no. 23: 12120–12130. https://doi.org/10.1002/2016GL070817.

Vonk, J. E., S. E. Tank, W. B. Bowden, et al. 2015. "Reviews and Syntheses: Effects of Permafrost Thaw on Arctic Aquatic Ecosystems." *Biogeosciences* 12, no. 23: 7129–7167. https://doi.org/10.5194/bg-12-7129-2015.

Walker, D. A., and K. R. Everett. 1987. "Road Dust and Its Environmental Impact on Alaskan Taiga and Tundra." *Arctic and Alpine Research* 19, no. 4: 479–489. https://doi.org/10.1080/00040851.1987.12002630.

Walker, D. A., and M. D. Walker. 1996. "Terrain and Vegetation of the Imnavait Creek Watershed." In *Landscape Function and Disturbance in Arctic Tundra*, edited by J. F. Reynolds and J. D. Tenhunen, vol. 120, 73–108. Springer. https://doi.org/10.1007/978-3-662-01145-4_4.

Walvoord, M. A., and B. L. Kurylyk. 2016. "Hydrologic Impacts of Thawing Permafrost—A Review." *Vadose Zone Journal* 15, no. 6: 1–20. https://doi.org/10.2136/vzj2016.01.0010.

Weidner, C. R., J. P. Zarnetske, A. D. Kendall, S. L. Martin, S. Nesheim, and A. J. Shogren. 2025. "Wetlands, Groundwater and Seasonality Influence the Spatial Distribution of Stream Chemistry in a Low-Relief Catchment." *Journal of Geophysical Research: Biogeosciences* 130, no. 8: e2025JG008989. https://doi.org/10.1029/2025JG008989.

Westermann, S., C. R. Duguay, G. Grosse, and A. Kääb. 2015. "Remote Sensing of Permafrost and Frozen Ground." In *Remote Sensing of the Cryosphere*, 307–344. John Wiley & Sons, Ltd. https://doi.org/10.1002/9781118368909.ch13.

Wilson, F. H., C. P. Hults, C. G. Mull, and S. M. Karl. 2015. *Geologic Map of Alaska (Scientific Investigations Map)*. U.S. Geological Survey Scientific Investigations Map.

Wollheim, W. M., C. J. Vörösmarty, B. J. Peterson, S. P. Seitzinger, and C. S. Hopkinson. 2006. "Relationship Between River Size and Nutrient Removal." *Geophysical Research Letters* 33, no. 6: L06410. https://doi.org/10.1029/2006gl025845.

Woo, M. 1983. "Hydrology of a Drainage Basin in the Canadian High Arctic." *Annals of the Association of American Geographers* 73, no. 4: 577–596. https://doi.org/10.1111/j.1467-8306.1983.tb01860.x.

Woo, M. 1986. "Permafrost Hydrology in North America." *Atmosphere-Ocean* 24, no. 3: 201–234. https://doi.org/10.1080/07055900.1986.9649248.

Woo, M., R. Heron, and P. Steer. 1981. "Catchment Hydrology of a High Arctic Lake." *Cold Regions Science and Technology* 5, no. 1: 29–41. https://doi.org/10.1016/0165-232X(81)90038-0.

Woo, M., and P. Steer. 1983. "Slope Hydrology as Influenced by Thawing of the Active Layer, Resolute, N.W.T." *Canadian Journal of Earth Sciences* 20, no. 6: 978–986.

Woo, M.-K., and P. Steer. 1982. "Occurrence of Surface Flow on Arctic Slopes, Southwestern Cornwallis Island." *Canadian Journal of Earth Sciences* 19, no. 12: 2368–2377. https://doi.org/10.1139/e82-206.

Woo, M.-K., and P. Steer. 1986. "Runoff Regime of Slopes in Continuous Permafrost Areas." *Canadian Water Resources Journal* 11, no. 1: 58–68. https://doi.org/10.4296/cwrj1101058.

Wood, S. 2020. *mgcv: Mixed GAM Computation Vehicle With Automatic Smoothness Estimation (Version 1.8-33)* [R]. https://CRAN.R-project.org/package=mgcv.

Wood, S. N. 2017. *Generalized Additive Models: An Introduction With R*. 2nd ed. Chapman and Hall/CRC. https://doi.org/10.1201/9781315370279.

Zahajská, P., C. Olid, J. Stadmark, S. C. Fritz, S. Opfergelt, and D. J. Conley. 2021. "Modern Silicon Dynamics of a Small High-Latitude Subarctic Lake." *Biogeosciences* 18, no. 7: 2325–2345. https://doi.org/10.5194/bg-18-2325-2021.

Zarnetske, J. P., M. N. Gooseff, W. B. Bowden, et al. 2008. "Influence of Morphology and Permafrost Dynamics on Hyporheic Exchange in Arctic Headwater Streams Under Warming Climate Conditions." *Geophysical Research Letters* 35, no. 2: L02501. https://doi.org/10.1029/2007gl032049.

Zarnetske, J. P., R. Haggerty, S. M. Wondzell, V. A. Bokil, and R. González-Pinzón. 2012. "Coupled Transport and Reaction Kinetics Control the Nitrate Source-Sink Function of Hyporheic Zones." *Water Resources Research* 48, no. 11: 2012WR011894. https://doi.org/10.1029/2012WR011894.

10991085, 2026, 4, Downloaded from https://onlinelibrary.wiley.com/doi/10.1002/hyp.70512 by Jonathan O'Donnell , Wiley Online Library on [17/09/2026]. See the Terms and Conditions (https://onlinelibrary.wiley.com/terms-and-conditions) on Wiley Online Library for rules of use; OA articles are governed by the applicable Creative Commons License

Zhi, W., and L. Li. 2020. "The Shallow and Deep Hypothesis: Subsurface Vertical Chemical Contrasts Shape Nitrate Export Patterns From Different Land Uses." *Environmental Science & Technology* 54, no. 19: 11915–11928. https://doi.org/10.1021/acs.est.0c01340.

Zhi, W., L. Li, W. Dong, et al. 2019. "Distinct Source Water Chemistry Shapes Contrasting Concentration-Discharge Patterns." *Water Resources Research* 55, no. 5: 4233–4251. https://doi.org/10.1029/2018WR024257.

Supporting Information

Additional supporting information can be found online in the Supporting Information section. **Table S1:** Mean, standard deviation (SD), median, and range of solute concentrations in the three study catchments. All values are in $mg\,L^{-1}$. Nearly all concentrations for Fe in the *Alpine* catchment were below detection and therefore are not included here.

10991085, 2026, 4, Downloaded from https://onlinelibrary.wiley.com/doi/10.1002/hyp.70512 by Jonathan O'Donnell , Wiley Online Library on [17/09/2026]. See the Terms and Conditions (https://onlinelibrary.wiley.com/terms-and-conditions) on Wiley Online Library for rules of use; OA articles are governed by the applicable Creative Commons License